



# 3D Printing Hydrogel for Flexible Mechanical Sensors

Dan Li<sup>1,\*\*</sup>, Lu Jiang<sup>1,\*\*</sup>, Zhiwei Sheng<sup>1</sup>, Yilin Wei<sup>1</sup>, Zhou Li<sup>2,3,†</sup>, Qiang Zheng<sup>1,†</sup>,

<sup>1</sup>Engineering Research Center for Bio-Perception Materials of Guizhou Province, Key Laboratory of Biology and Medical Engineering/Immune Cells and Antibody Engineering Research Center of Guizhou Province, and Engineering Research Center of Intelligent Materials and Advanced Medical Devices, School of Biology and Engineering, Guizhou Medical University, Guiyang 550025, China

<sup>2</sup>Vita Tech Innovation Center, Tsinghua Changgung Hospital, School of Clinical Medicine, Tsinghua University, Beijing 100084, China

<sup>3</sup>School of Biomedical Engineering, Tsinghua University, Beijing 100084, China

\*\*These authors contributed equally.

†E-mail: li\_zhou@tsinghua.edu.cn(Z.L.), zhengqiang@gmc.edu.cn(Q.Z.)

Received: October 28, 2025 / Revised: January 4, 2026 / Accepted: January 16, 2026 / Published online: January 31, 2026

**Abstract:** The growing demand for flexible sensors, driven by advances in flexible electronics, highlights hydrogels as an ideal material due to their intrinsic flexibility, biocompatibility, and multifunctional sensing capabilities. The fabrication of hydrogel devices with complex three-dimensional (3D) architectures and customized functions remains a challenge for traditional methods, while the limitation is now being overcome by 3D printing technology. Compared with 3D bioprinting, which has entered an advanced stage of development and 3D printing of plastics, metals, and resins, where technologies are relatively mature, 3D printing of hydrogel devices is still in the middle exploration stage. In this review, we mainly introduce recent progress on how to use 3D printing to build high-performance flexible electronic devices based on hydrogels, from the perspective of regulating key 3D printing process parameters. We emphasize the influence of material parameters, process parameters, and post-processing on device performance. We explain the working principles, performance indicators, and material characteristics of mainstream sensors such as resistive sensors, introduce various 3D printing methods for hydrogels, then discuss the ink design principles and the balance between printing quality and printing functions, and summarize the latest progress of these sensors in health monitoring, motion detection, and human-machine interaction. In short, this article looks forward to the future development direction of this attractive field.

**Keywords:** 3D Printing; Hydrogel; Sensor; Health Monitoring; Human-Machine Interaction; Motion Detection

<https://doi.org/10.64509/jim.11.43>

## 1 Introduction

With the advent of the intelligent era, flexible sensors have garnered significant attention for the fabrication of medical-monitoring devices, intelligent robots, and wearable electronics [1–4]. Sensing material is the decisive factor that governs how well these functions can be realized. The materials currently in common use for flexible sensors, such as polymeric elastomers and silicone rubbers, are subject to several limitations [5, 6]. First, their poor biocompatibility and limited skin adaptability often provoke irritation or allergic reactions when worn for long periods. Second, the structural non-uniformity of conventional multilayer sensors frequently leads to delamination and consequent device failure. Finally, the modulus mismatch at the mechanical interface causes interface failure, restricting the large-deformation compliance required of

stretchable electronics and giving rise to motion artifacts that compromise signal fidelity [7–9]. In this scenario, hydrogels bear a resemblance to the physiological structure of soft tissues, a characteristic that renders them exceptionally valuable across biomedical and bioengineering domains [10, 11]. Secondly, hydrogels can achieve tunable conductivity by incorporating ions or other methods. Additionally, their flexibility can be adjusted by modifying crosslinking density, polymer type, and molecular weight [12]. Finally, the abundant water content, smart responsiveness, and antibacterial/anti-fouling properties within hydrogel networks further enhance their versatile applications across diverse scenarios [2, 13].

Despite significant breakthroughs in hydrogel applications across various fields, non-negligible limitations have gradually emerged. First, Hydrogels fabricated through manual handling or conventional casting methods are highly

† Corresponding author: Zhou Li, Qiang Zheng

\* Academic Editor: Yannan Xie

© 2026 The authors. This article is an open access article distributed under the terms and conditions of the Creative Commons Attribution (CC BY) license (<https://creativecommons.org/licenses/by/4.0/>).

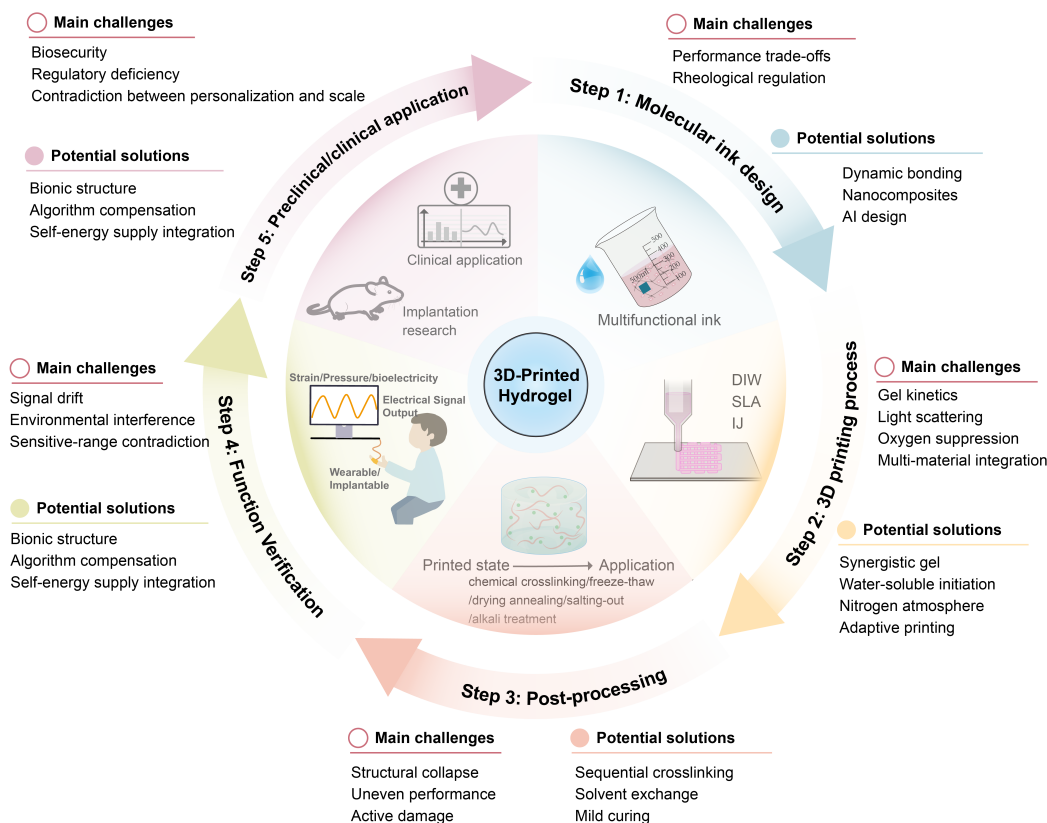


**Figure 1:** The Process for Developing 3D-Printed Hydrogel-Based Flexible Sensors.

susceptible to human factors and reaction condition fluctuations. Besides, current gelation techniques often take time, require much labor, waste materials, and have low scalability. More critically, the molding process is constrained by molds or containers, making it difficult to achieve precise fabrication of complex 3D microstructures. In contrast, 3D printing, a rapid prototyping technology also known as additive manufacturing (AM), is a “bottom-up” fabrication approach that enables the creation of physical objects through layer-by-layer material deposition. This method allows for precise control over design and manufacturing parameters, facilitating the development of objects with tailored shapes, dimensions, architectural complexity, and microstructural environments [14]. Furthermore, this approach enables the utilization of diverse material systems ranging from metals to polymers, thereby facilitating the fabrication of objects with tailored physicochemical properties [15]. Moreover, it significantly reduces both temporal and material resource expenditures in fabricating target objects. Capitalizing on these compelling advantages, 3D printing is instigating a global paradigm shift across diverse sectors, including medical technology, biomedical engineering, and electronic device manufacturing [16, 17].

3D printing of hydrogels represents an emerging technology that synergizes the unique properties of hydrogel materials with the advantages of additive manufacturing, enabling the fabrication of hydrogel products with precisely controlled geometries and architectures [18–20]. Compared with the well-studied 3D bioprinting, research on 3D printed hydrogel-based flexible sensors has not fully explored key

aspects like material preparation, ink formulation, and device design, and their practical applications are still in the early stages. This challenge mainly stems from the inherent conflict between the printability requirements of 3D printed hydrogel devices and their desired performance. For example, insufficient mechanical strength and structural stability, low electrical conductivity and printing resolution, poor printability, and structural fidelity [21]. A critical challenge is the poor interfacial adhesion when integrating different printed components into unified structures: brittle hydrogels have inadequate bonding strength, and interfacial cracks readily propagate to cause cohesive failure, which requires enhanced material toughness to dissipate mechanical energy and suppress crack propagation [16].

Therefore, this review presents a comprehensive overview of recent advancements in 3D-printed hydrogel-based flexible mechanical sensors. Figure 1 schematically illustrates the entire development pipeline addressed in this review, encompassing molecular ink design, 3D printing processes, post-treatment strategies, functional validation, and translational applications, with key challenges and corresponding mitigation strategies annotated at each stage. In the main text, we first systematically introduce the working principles and essential performance metrics of flexible mechanical sensors. Subsequently, we examine various 3D printing techniques applicable to hydrogel fabrication. This is followed by an in-depth analysis of ink design principles, with particular emphasis on the critical influence of hydrogel rheology on printability. The review further highlights recent breakthroughs in application areas such as human health monitoring, motion detection, and human-machine interaction. Finally, we

critically evaluate existing challenges and propose promising future research directions to advance the field.

## 2 Overview of Different Sensors

Mechanical sensors can provide important information and insights into individual health status, physiological characteristics, and human–machine interaction. Based on the principles of operation, mechanical sensors can be categorized into resistive, capacitive, piezoelectric, and triboelectric sensors. The mechanisms, advantages, disadvantages, and representative sensing materials of these sensors are shown in Figure 2.

### 2.1 Resistive Sensors

As the most widely used type of sensor, piezoresistive force sensors are highly sensitive to changes in pressure and vibration. The fundamental principle of piezoresistive sensors is to detect the changes in resistance and current of the conductive material within the sensor under the stimulation of external stress. The resistance of the conductive material can be expressed as:

$$R = \rho \frac{L}{S} \quad (1)$$

As defined, when the structure of the sensor undergoes deformation, the length  $L$  and cross-sectional area  $S$  of the conductive material will change correspondingly, leading to a variation in the sensor's resistance  $R$ . This principle is the basis for fabricating some traditional rigid strain sensors, such as metal strain gauges. For traditional rigid sensors, sensitivity is the most crucial performance metric, in addition to other important characteristics such as cyclic stability, hysteresis, and response time. The sensitivity of a piezoresistive force sensor is defined as the ratio of the relative resistance change ( $\Delta R/R_0$ ) to the applied pressure ( $P$ ). Therefore, the sensitivity, often represented as gauge factor ( $GF$ ), can be expressed as follows:

$$GF = \frac{\Delta R}{R_0} \frac{1}{P} \quad (2)$$

It can be seen that the  $GF$  (gauge factor) represents the slope of the curve of relative resistance change of the sensor versus the applied strain. Therefore, the higher the  $GF$  of a sensor, the greater the resistance change of the material, which means the material is more sensitive to external forces. Thus, high sensitivity has always been a key pursuit in the design of conductive materials for sensors. The integration of conductive components (such as carbon-based materials, metallic nanomaterials, and conductive polymers) with flexible polymer matrices (such as polyacrylonitrile (PAN), polyurethane (PU), and polydimethylsiloxane (PDMS)) results in flexible conductive polymer composites that combine conductivity and stretchability. These sensors are particularly suitable for strain and deformation measurement, such as in wearable motion monitoring (e.g., joint bending, skin stretch) and structural health sensing, where resistance changes correlate directly with mechanical strain.

For piezoresistive force sensors, another critical metric is the pressure response range within which they can operate stably. The wide linear response characteristic of piezoresistive

sensors is typically achieved by optimizing the types of elastic matrices and conductive materials [22, 23]. Additionally, it is necessary to conduct microstructural design (e.g., micro-cylinders, micro-pyramids, and microcubes) of the matrices and materials based on the characteristics and mechanisms of the sensors, which can enhance the performance of sensitivity, detection limit, and response time [24–27].

### 2.2 Capacitive Sensors

The core component of a capacitive sensor is the capacitor, whose capacitance varies with changes in the spacing between the plates, the plate area, or the dielectric constant. These changes may originate from the physical quantity being measured, such as displacement, pressure, liquid level, or humidity. The capacitance of a capacitive sensor can be expressed as follows:

$$C = \frac{\epsilon S}{d} \quad (3)$$

Here,  $C$  represents the capacitance between the metal plates,  $\epsilon$  is the dielectric constant of the medium between the plates,  $S$  denotes the effective relative area between the plates, and  $d$  is the distance between the plates. For devices composed of flexible materials, all three of these variables are susceptible to changes in pressure. Therefore, pressure can be measured by observing the changes in the capacitive signal. The sensitivity of a capacitive pressure sensor is defined as the ratio of the relative capacitance change ( $\Delta C/C_0$ ) to the applied pressure. Thus, the sensitivity, often denoted as  $K$ , can be expressed as follows:

$$K = \frac{\Delta C}{C_0} \frac{1}{P} \quad (4)$$

Compared with resistive sensors, capacitive sensors typically exhibit higher sensitivity and lower detection limits, and have achieved a new level of performance, enabling applications that were previously unattainable with existing piezoresistive technologies. Due to their high sensitivity and low detection limit, capacitive sensors are ideal for measuring gentle pressure and subtle tactile signals, such as in touch interfaces, pulse wave monitoring, and light-touch detection in robotic skin. However, their relatively poor linear response, as well as their susceptibility to parasitic and fringing capacitances, can pose challenges in practical applications [28].

It is worth noting that the dielectric layer is a crucial target for optimizing the sensitivity and pressure response range of capacitive pressure sensors. Due to the incompressibility of soft materials, the sensitivity of the device is extremely low without the introduction of special structures. Therefore, forming special microstructures, such as spherical, cylindrical, and conical shapes, by introducing a second phase can significantly enhance the sensitivity of capacitive pressure sensors [29]. Additionally, using highly elastic materials to introduce air gaps or fabricating the dielectric material into porous foam-like structures can also greatly improve the sensitivity of capacitive pressure sensors [30, 31].

Regarding the material selection for the two electrodes, traditional electrodes are typically made of rigid materials

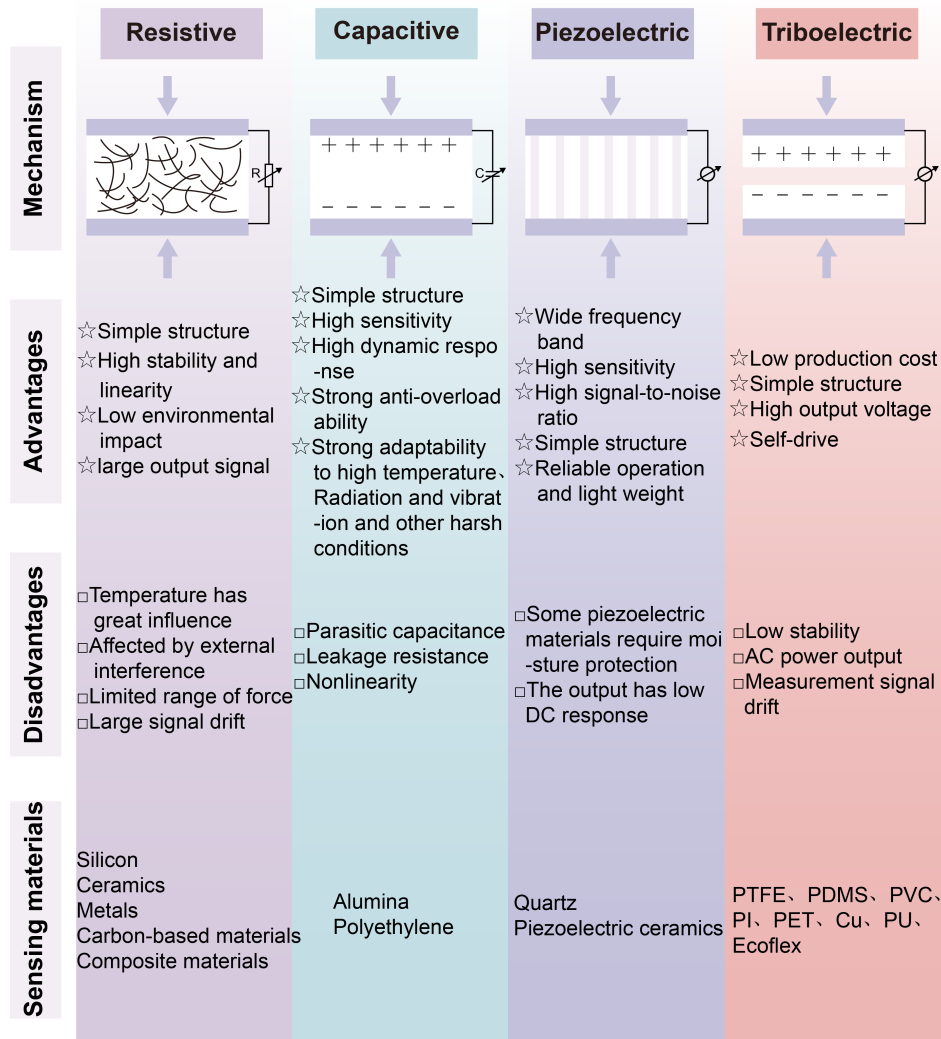


**Figure 2:** Features of the most commonly used flexible mechanical sensors.

such as metals and semiconductors. When subjected to external forces, the significant difference in Young's modulus between the dielectric layer and the electrodes often leads to interface detachment, thereby altering the structure of the capacitive sensor and affecting its sensing and detection values. Flexible and stretchable materials due to their important role in flexible electronics. These include highly conductive materials such as silver nanowires, carbon nanotubes, combined with flexible PDMS to form transparent stretchable composites. The combination of conductive liquids and polymer composites to form low-resistance gels also shows great potential. These novel materials, with their excellent electrical conductivity, sensitivity, and fast response characteristics, have demonstrated significant application potential as flexible electrode materials in the field of capacitive force sensors [32–34].

### 2.3 Tribo/Piezoelectric Sensors

Utilizing the variation of resistance and capacitance to convert pressure signals into electrical signals is a common method in mechanical sensors. After decades of development, these sensors have met the requirements of medical detection and motion monitoring in terms of sensitivity, response range, and linearity. However, a major limitation of these sensors

is that they still require an external power source to achieve signal conversion. The reliance on external power not only increases the complexity of the device but also poses significant challenges for integrating flexible sensing components with power supply devices. To meet the demand for self-powered capabilities, recent research has shifted towards triboelectric and piezoelectric sensors [35]. These sensors are especially well-suited for detecting dynamic or vibrational mechanical signals, such as body movement, heartbeat, voice vibration, and impact sensing, owing to their ability to directly convert mechanical energy into electrical signals without an external power source.

In triboelectric sensors, the working mechanism is based on the coupling effect of triboelectrification and electrostatic induction. Two dielectric materials with different electronegativities are compressed to generate triboelectric changes at the interface. After the applied force is released, the separation between the two layers creates an electric potential difference, thereby achieving self-powered operation. Depending on the electrode configuration and operating mode, triboelectric nanogenerators (TENGs) can be categorized into four main types: vertical contact-separation mode, contact-sliding mode, single-electrode mode, and freestanding triboelectric layer mode [36]. In sensor applications, the most commonly used mode is the vertical contact-separation mode.

Piezoelectric sensors are devices that utilize the piezoelectric effect of piezoelectric materials to achieve detection. When certain dielectric materials are subjected to an external force along a specific direction, they deform and undergo internal polarization, resulting in the generation of polarization charges. As the external pressure increases, the density of these polarization charges also increases correspondingly. By connecting an external load, an electric current is formed between the electrodes. The variation in this current is directly related to the applied pressure, thereby enabling the sensing function [37]. However, the choice of suitable piezoelectric materials is primarily limited to piezoelectric ceramics (such as barium titanate, lead zirconate titanate, ZnO, and polyvinylidene fluoride (PVDF)) and crystals (such as quartz). Traditional thin films based on inorganic composite piezoelectric materials face issues such as defects, cracks, and poor dispersion, which have become a bottleneck hindering the development of piezoelectric sensors [38, 39].

Similar to other types of sensors, a potential solution to these issues currently lies in integrating advanced composite materials and microstructural designs into traditional conductive materials [39–42]. However, the sensors obtained not only fail to have their performance adjusted according to practical needs, but also encounter difficulties in precisely controlling their structural design [43–45]. In recent years, with the continuous development of 3D printing technology, the rapid and efficient fabrication of functional, high-resolution, and customizable hydrogels has attracted widespread attention [46–48]. Figure 3 summarizes the latest research on developing mechanical sensors using traditional materials and indicates the recent shift towards using 3D printing technology for creative, customized, and rapid prototyping of multi-material and customized mechanical sensors.

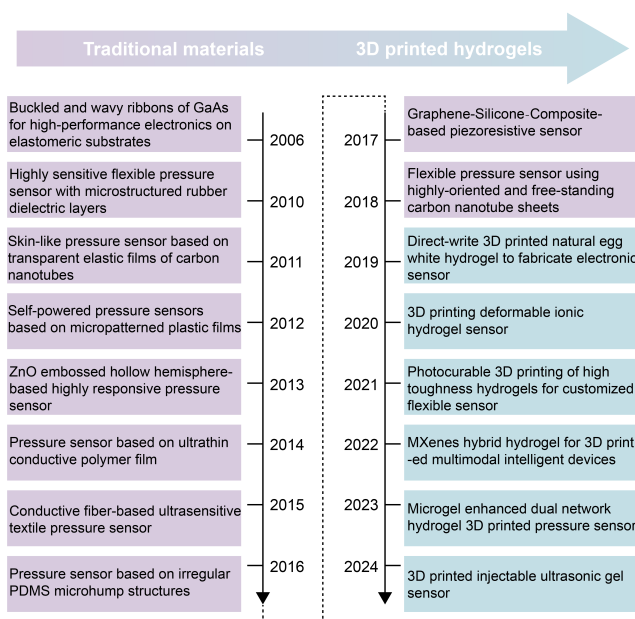


**Figure 3:** Summary of state-of-the-art studies in which sensors were fabricated using conventional and 3D printing techniques [49–64].

### 3 Commonly Used 3D Printing Techniques for Hydrogels

3D printing is a process that fabricates objects by incrementally stacking materials layer by layer to construct complex shapes [65]. Initially, CAD modeling of the object to be printed is performed using computer-assisted devices. The 3D digital model is then converted into the STL format and subjected to slicing processing. Subsequently, the computer controls the printer to level the platform and feed the material. Finally, each slice is printed in sequence. By following this procedure and stacking layer by layer, the entire model is gradually constructed until the printing is completed. In addition to the aforementioned steps, the printed object requires relevant post-processing to obtain a qualified model [66]. A variety of techniques have been employed for printing hydrogels and their composites, such as Direct Ink Writing (DIW), Inkjet Printing (IJ), and Stereolithography (SLA). This section focuses solely on the commonly used 3D printing techniques for hydrogels.

#### 3.1 Direct-Ink Writing 3D Printing

DIW, also known as direct writing, is a method associated with material extrusion. Extrusion-based printing is a common 3D printing technique. Initially, the 3D printer converts a three-dimensional digital model into G-code and transmits it to the printer controller. Subsequently, the printer extrudes and deposits the fluid, viscoelastic hydrogel-based ink onto the build platform through a syringe or mobile nozzle, driven by pneumatic or mechanical forces. After each layer is deposited, the build platform descends by a specific distance, and the nozzle proceeds to deposit the next layer of material [67]. This process continues iteratively until the entire model is completed, as illustrated in the left half of Figure 4. After deposition is complete, the printed object can be subjected to post-curing treatment through heating or ultraviolet (UV) irradiation. A variety of factors, such as the viscosity and density of the ink, the diameter and geometry of the nozzle, the printing speed, and the applied pressure, all significantly influence the performance and surface accuracy of the final model [68]. The specific viscosity and fluidity required for hydrogel ink before crosslinking are the key to resolving the “contradiction between printability and performance” through rheological regulation. Appropriate fluidity ensures that the ink can be smoothly extruded and continuously formed, meeting the basic requirements of printability. The remarkable shear thinning and rapid recovery capabilities enable the sedimentary structure to maintain its shape and resist collapse, thereby ensuring geometric accuracy and interlayer bonding, and directly addressing the challenges of structural integrity and interface bonding. Slow gelation can lead to feature sagging or fusion between adjacent filaments, while excessively rapid gelation may cause nozzle clogging or hinder interlayer adhesion. Therefore, the precise design of the ink’s viscous flow characteristics is essentially aimed at achieving a reliable transformation from “printable fluid” to “high-performance solid, thereby simultaneously realizing the feasibility of processing and the construction of functional structure during the printing process. Compared to other 3D

printing techniques, hydrogels and their composite materials can be processed using DIW as long as they meet the required viscosity and rheological properties, thereby offering a certain degree of flexibility in the choice of raw materials [69]. Moreover, one of the principal advantages of DIW is that material deposition can occur at ambient temperature, thereby eliminating the influence of thermal and residual stresses on the printed model. This feature helps mitigate the issue of interfacial delamination caused by thermal mismatch, which is a key challenge in integrating multiple printed components.

### 3.2 Inkjet 3D Printing

IJ is a 3D printing process that was developed relatively early. As shown in Figure 4, in an inkjet printing system, minute droplets of hydrogel ink are deposited onto a substrate and solidified. Utilizing photosensitive polymers that cure upon exposure to UV light [70]. The nature of the material jetting process allows for the deposition of different materials on the same object. IJ 3D printing technology primarily encompasses two approaches: continuous inkjet printing and drop-on-demand (DOD) inkjet printing [71]. Continuous inkjet printing involves the ejection of ink through a nozzle under pressure, with ink droplets being deflected using an electric field or other means. Unused droplets can be recycled. This method is characterized by its high speed and precision but suffers from complex equipment requirements and stringent ink limitations, making it commonly used for rapid prototyping in industrial manufacturing. In contrast, DOD inkjet printing systems deposit precursor ink in the form of individual droplets, with a predetermined volume of ink driven by thermal or piezoelectric devices. The advantages of DOD printing include ink conservation and high flexibility, although it is relatively slower and more prone to nozzle clogging. It is widely applied in fields that demand a high degree of material diversity.

Extrusion Printing	Inkjet Printing	Stereolithography
<p><b>Advantages</b></p> <ul style="list-style-type: none"> <li>Simple, low cost,</li> <li>Multi-material ability</li> <li>Rapid print speed</li> <li>High resolution</li> </ul> <p><b>Disadvantages</b></p> <ul style="list-style-type: none"> <li>Nozzle clogging</li> <li>post-curing</li> <li>Rheology control</li> <li>Low resolution</li> </ul> <p><b>Ink Material Requirements</b></p> <ul style="list-style-type: none"> <li>Shear-thinning properties</li> <li>High elastic modulus</li> <li>Functional additives</li> </ul>	<p><b>Advantages</b></p> <ul style="list-style-type: none"> <li>High resolution, high speed</li> <li>High cell viability</li> <li>Multi-material ability</li> <li>Inexpensive hardware</li> </ul> <p><b>Disadvantages</b></p> <ul style="list-style-type: none"> <li>Complex ink properties and post-processing</li> <li>Slow print speeds</li> <li>Limited structural complexity</li> </ul> <p><b>Ink Material Requirements</b></p> <ul style="list-style-type: none"> <li>Low viscosity</li> <li>Surface tension</li> <li>Rapid curing</li> </ul>	<p><b>Advantages</b></p> <ul style="list-style-type: none"> <li>High resolution</li> <li>Multi-material ability</li> <li>Nozzle-free fabrication</li> <li>Rapid print speed</li> <li>Can form complex architectures</li> </ul> <p><b>Disadvantages</b></p> <ul style="list-style-type: none"> <li>High cost, slow, and material limitations</li> <li>Limited multimaterial functionality</li> <li>Cumulative UV exposure</li> </ul> <p><b>Ink Material Requirements</b></p> <ul style="list-style-type: none"> <li>Photocuring capability</li> <li>Transparency</li> <li>Low viscosity</li> <li>Biocompatibility</li> </ul>

**Figure 4:** Main characteristics of 3D printing techniques.

The key to successful IJ 3D printing lies in the nozzle technology, ink performance, and the printing control system. Precision control, ejection frequency, and stability are

crucial for nozzle technology, as these factors determine the size of the ink droplets, their ejection position, printing speed, and overall print quality. Additionally, the viscosity and fluidity of the ink, its drying speed, and the compatibility of its chemical composition significantly influence droplet formation, ejection, and the compatibility of the ink with the nozzle and printing substrate [72]. It should be particularly noted that IJ 3D printing has extremely strict requirements for the viscosity and fluidity of hydrogel ink, which is essentially determined by its principle of micro-scale droplet formation and deposition. The viscosity must be precisely controlled within a relatively low range (typically 3–30 mPa·s) to ensure that the droplets can form smoothly and be stably ejected without breaking or splashing. At the same time, the ink needs to have appropriate fluidity (especially surface tension) to ensure the wettability after droplet drop, shape retention, and interlayer stacking accuracy. These constraints not only limit the range of available materials, but also highlight the inherent contradiction between "printability" and "material functionality" in high-resolution printing: To achieve fine molding, ink often needs to sacrifice a certain amount of solid content, filler load, or crosslinking density, which may affect the mechanical, electrical, or biological properties of the final device. Additionally, the printing control system ensures printing efficiency and quality through precise path planning and flexible parameter adjustment [73]. Compared with extrusion-based 3D printing, Inkjet (IJ) printing can achieve higher resolution and finer structural details. It allows on-demand ejection of materials, resulting in minimal waste and the ability to rapidly switch between multiple materials, which is advantageous for fabricating complex structures. Moreover, nozzle clogging may occur during the printing process, affecting the stability and continuity of printing. This operational challenge further emphasizes the need for robust material formulations to ensure reliable device fabrication.

### 3.3 Stereolithography 3D Printing

Stereolithography (SLA) is the earliest 3D printing technology to be commercialized and widely applied. After years of development, SLA 3D printing technology has become one of the most mature technologies in the field today. As shown in the right half of Figure 4, the SLA technology is based on the principle of photopolymerization and utilizes liquid photosensitive resin as the raw material. During the printing process, UV light selectively irradiates the surface of the liquid photosensitive resin according to the two-dimensional pattern information derived from the sliced CAD model. The photoinitiator in the resin, upon absorbing the energy of UV light at a specific wavelength, generates reactive species that trigger the polymerization reaction between monomers, rapidly converting the liquid resin into a solid state. Initially, the printing platform is positioned close to the surface of the liquid resin. After one layer is cured, the platform descends by a certain distance (typically with a layer thickness ranging from 25 to 100 micrometers). Fresh liquid resin then covers the cured layer, and the UV light continues to irradiate and cure the next layer according to the subsequent pattern. This process is repeated layer by layer until the complete three-dimensional model is constructed [74]. The apparatus consists

of a light source (system such as a laser or digital light projector), a resin vat, a printing platform, as well as a control system and software.

Among the several widely-used rapid prototyping processes, photopolymerization-based additive manufacturing is extensively applied across various scenarios due to its high degree of automation, superior surface quality of the prototypes, high dimensional accuracy, and the ability to achieve fine-scale feature fabrication. To control the curing time and printing quality, it is essential to optimize parameters such as laser power intensity, exposure duration, and scanning speed. When printing with hydrogel precursors, which are predominantly water-based, two phenomena specific to the aqueous environment critically influence the process: light scattering and oxygen inhibition. Light scattering by water molecules and dissolved components can reduce the effective resolution and cure precision, especially when attempting to fabricate fine features. More notably, at the vital air-resin interface (the open surface), oxygen diffusion competitively quenches the photoinitiated radicals, a process known as oxygen inhibition. This can lead to incomplete surface curing, resulting in tacky layers and compromised mechanical integrity of the top-most structures. Addressing these challenges often requires tailored strategies, such as optimizing photoinitiator systems for aqueous media, employing water-soluble co-initiators or oxygen scavengers, and, in some cases, implementing controlled atmosphere printing (e.g., nitrogen purging) to mitigate surface inhibition. Material selection and performance are also critically important. High-quality photosensitive resins should possess appropriate viscosity, curing rate, and shrinkage, and must be matched to specific application scenarios. Finally, post-processing techniques must not be overlooked. These include cleaning to remove residual resin, carefully removing supports, and conducting secondary curing, as well as finishing operations such as grinding and polishing to enhance the performance and appearance of the printed parts [75].

## 4 Design Strategy of 3D Printing Hydrogel Ink

### 4.1 Hydrogel Precursor

Hydrogels are three-dimensional polymeric networks capable of absorbing large amounts of water and biological fluids. These networks are formed by physical and chemical covalent bonds between synthetic chains and contain hydrophilic groups, which can provide a hydrophilic environment for cells [76]. Materials are the foundation of sensor performance, so

it is essential to analyze the relationship between the composition design and the functions of hydrogels. This section will explain the design principles of hydrogel precursors by starting with the hydrogel matrix materials, supplementing with functional modification strategies, while also summarizing their respective advantages, disadvantages, and the latest research progress. Table 1 intuitively summarizes the main characteristics of different hydrogel substrates.

#### 4.1.1 Hydrogel Matrix

Based on the source of the matrix materials, hydrogels can be classified into natural polymer-based hydrogels, synthetic polymer-based hydrogels, and hybrid polymer-based hydrogels. Natural hydrogels are synthesized from natural polymers and exhibit several desirable properties, including biodegradability, biocompatibility, bio-molecular recognition, high availability, and low cost. The raw materials for natural polymer-based hydrogels primarily include various polysaccharides and proteins. Common natural polymers encompass sodium alginate, chitosan, hyaluronic acid, and others [77].

The advantages of natural biomaterials stem from their excellent biocompatibility, which enables them to adapt well to the human body environment. Among the numerous polymers used for hydrogel printing inks, alginate is one of the most commonly used materials. Alginate possesses good biocompatibility, biodegradability, ease of functionalization, and rapid gelation behavior, making it an ideal material for bioinks [78–80]. In addition to polysaccharides, proteins are also widely used as materials in 3D-printable hydrogel inks. Peptide hydrogels are characterized by their high water content, porous structure, tunable mechanical stability, excellent biocompatibility, outstanding injectability, and elasticity similar to that of natural tissues. Moreover, their degradation produces only amino acids, which are relatively safe for the body. Therefore, 3D printing using protein-based inks holds great application potential [81].

Synthetic polymer hydrogels are hydrogels formed by the crosslinking of synthetic hydrophilic polymers through physical or chemical interactions. Commonly used synthetic polymers include polyethylene glycol (PEG), polydopamine (PDA), and polyvinyl alcohol (PVA). Synthetic polymer hydrogels can control their mechanical properties by changing their ingredients and crosslinking. This includes elasticity, toughness, and recovery [82, 83]. Second, they can be chemically modified to add functional groups or nanoparticles [84, 85]. Compared with natural hydrogels, synthetic hydrogels typically exhibit superior chemical stability. This

**Table 1:** Properties of Matrix Hydrogels from Different Sources

Hydrogel matrix	Typical Materials	Core Advantages	Limitations
Natural polymer-based hydrogels	Sodium Alginate, Gelatin, Chitosan	Good Biocompatibility, Biodegradability	Low Mechanical Strength, Poor Stability
synthetic polymer-based hydrogels	Poly(N-isopropylacrylamide) (PNIPAM), Polyvinyl Alcohol (PVA)	Tunable Mechanical Properties, High Chemical Stability, Clear Stimuli-Responsiveness	Biocompatibility Needs Optimization
hybrid polymer-based hydrogels	Doped Nanofillers (CNT, Graphene), Fibers (Bacterial Cellulose)	Enhanced Electrical Conductivity, Mechanical Strength, and Sensing Sensitivity	Poor Filler Dispersion, Impaired Printability

stability ensures the long-term reliability of biomechanical sensors.

When developing 3D-printable hydrogels for biomechanical sensing, several synthetic polymers are widely utilized. PEG has emerged as a popular choice due to its biocompatibility, non-toxicity, and ease of functionalization. Another commonly used synthetic polymer is polyacrylic acid (PAA), which forms hydrogels with high water absorption capacity and tunable mechanical properties. The strength and stability of PAA hydrogels can be further enhanced by incorporating crosslinking agents. In addition, PVA hydrogels have been extensively studied for their excellent mechanical properties and biocompatibility [86]. PVA hydrogels can be prepared through freeze-thaw cycles or chemical crosslinking, resulting in materials with adjustable stiffness and elasticity. Despite the numerous advantages of synthetic hydrogels, they still face several challenges in the context of 3D printing and biomechanical sensing. One major issue is that certain synthetic polymers and crosslinking agents may exhibit cytotoxicity, which must be carefully considered in applications involving direct contact with biological tissues. Moreover, the complex rheological properties of some synthetic hydrogels can pose challenges for 3D printing, necessitating the optimization of printing parameters and ink formulations to achieve high-fidelity structures [87–89].

Hybrid hydrogels are made from two or more different types of natural/synthetic polymers or nanofillers. They combine the benefits of both natural and synthetic polymer hydrogels, offering good biocompatibility and mechanical properties. As a result, their use in skin tissue engineering has grown rapidly in recent years. For example, hydrogels combining hyaluronic acid and PEG have been developed.

In conclusion, the selection of 3D-printable hydrogel inks should be determined based on the characteristics of the materials, the requirements of the printing technology, and the demands of the final application. Besides the principles for matrix materials, the crosslinking methods of hydrogels should also be taken into account. Chemical crosslinking is suitable for applications that require rapid curing and high mechanical strength [90–92], whereas physical crosslinking is more appropriate for scenarios that demand biocompatibility and reversibility [87, 88, 93, 94]. A dual-crosslinking strategy combines the advantages of both approaches, offering more flexible performance tuning.

#### 4.1.2 Functionalization Strategies

While the hydrogel matrix provides the foundational framework for 3D printability and biocompatibility, its intrinsic properties are often insufficient for the core requirements of flexible sensors: signal transduction, mechanical robustness, and stimulus responsiveness. Consequently, targeted functional modifications are essential. This section discusses strategies to improve these critical functionalities, while also highlighting the inherent trade-offs that accompany each design choice, as optimizing one property often compromises another. These interconnected trade-offs between conductivity, transparency, printability, and biocompatibility underscore the need for carefully balanced ink design, as illustrated conceptually in the performance trade-off network (Figure 5).

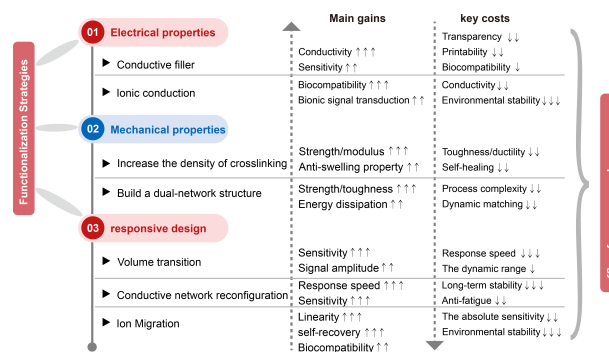


**Figure 5:** Overview of trade-offs in functionalization design for 3D-printed hydrogels.

Conductive modification is essential to enable the conversion of mechano-electric transduction. Since most hydrogel matrices are electrical insulators, incorporating conductive components is necessary to establish percolating conductive networks. Commonly used fillers include carbon-based nanomaterials (e.g., graphene, carbon nanotubes), metal-based materials (e.g., silver nanowires, gold nanoparticles), and conductive polymers (e.g., PEDOT: PSS, polyaniline) [87, 93]. These fillers are introduced primarily via two methods: physical blending or chemical grafting. Physical blending is straightforward but often results in unstable conductive networks due to filler aggregation and migration, leading to signal drift. In contrast, chemical grafting covalently anchors conductive components to the polymer backbone, creating a more uniform and durable network that withstands repeated deformation. Crucially, the introduction of conductive fillers often involves navigating a network of performance trade-offs. High transparency of hydrogels can be maintained when the fillers are nanoscale and uniformly dispersed. However, the transparency of hydrogels will decrease significantly once the fillers are poorly dispersed and agglomerated, or the refractive index difference between the fillers and the matrix is significant, and the higher the amount of fillers added, the more obvious the decrease in transparency. This is a critical property for applications that require visual observation of devices or optical interfacing. High filler loadings may also deteriorate the rheological properties of the ink, impairing printability by increasing viscosity or inducing abnormal shear thinning, which affects the structural fidelity in 3D printing. In addition, if the fillers are unevenly dispersed to form large aggregates, they may not only clog the print nozzles but also lead to uneven performance distribution of the printed parts, resulting in differences in strength and conductivity in different parts, thus affecting the quality of the finished products. The biocompatibility and degradability of hydrogels may also be affected by the type, concentration, and potential leaching risk of fillers. Toxic or easily agglomerated fillers may damage cells and further induce inflammation, and the degradation rate of degradable hydrogels may be affected by fillers. For in vivo applications, the biocompatibility of fillers directly affects the tissue integration effect, and suitable fillers can also assist in the electrical signal conduction related to nerve repair.

Mechanical enhancement matches reliability under dynamic conditions. The inherent mechanical weakness and brittleness of many hydrogels limit their durability under

repeated stress. Several strategies have been developed to enhance their mechanical properties. Double-network (DN) hydrogels combine a rigid, brittle first network with a soft, ductile second network [44, 45]. When the rigid but brittle first network is subjected to stress, the sacrificial bonds within it (such as ionic bonds, hydrogen bonds, or reversible covalent bonds) will break preferentially. This process irreversibly consumes a large amount of mechanical energy and greatly enhances the fracture toughness of the material. The flexible and highly entangled second network, while partially sacrificing the first network, continues to extend highly and bear the load, preventing a catastrophic overall fracture caused by local damage. The structure of the two networks interpenetrating not only endows the hydrogel with unprecedented high strength and high toughness, but also fundamentally improves its fatigue resistance and long-term cycling stability. Under cyclic loading, damage (sacrifice bond breakage) can be confined locally and not accumulate, while the overall structural integrity is maintained. This is precisely the key materials science strategy to solve the long-term stability problems of flexible sensors, such as interface delamination and signal drift during dynamic use. Nanocomposite reinforcement incorporates nanofillers (e.g., halloysite nanotubes, cellulose nanofibers) that act as multifunctional physical cross-links, enhancing modulus and toughness by efficiently distributing stress. This strategy enhances interfacial bonding between the hydrogel matrix and fillers, reducing the risk of delamination and cohesive failure. On the one hand, high modulus fillers directly bear stress and increase the network crosslinking density, significantly enhancing the material stiffness; On the other hand, the filler achieves multiple energy dissipation through mechanisms such as inducing crack deflection, interface debonding, and pulping, effectively enhancing toughness. Meanwhile, the optimized filler-matrix interface ensures the efficient transmission of stress, preventing the interface from becoming a weak point in the structure, thereby significantly suppressing delamination and cohesion failure, and enhancing the durability and structural reliability of the material under cyclic loading. Furthermore, precise control of chemical cross-linking density is crucial. It balances elasticity and strength to prevent brittleness or softness [43, 46]. However, a fundamental trade-off exists between strength (or modulus) and toughness (or stretchability). Increasing the chemical cross-linking density effectively enhances the hydrogel's stiffness and tensile strength but simultaneously reduces the network's ability to dissipate energy through chain mobility or sacrificial bond rupture, often leading to embrittlement and lower fracture toughness. This inverse relationship is a central challenge in designing hydrogels that are both strong and tough, akin to many natural tissues. The goal of these strategies is to match the mechanical properties of hydrogels with human tissues and ensure reliable performance under dynamic loading.

Through responsive design, specific mechanisms can be tailored to distinct mechanical stimuli. The sensitivity and specificity of hydrogel-based sensors are fundamentally governed by their responsive mechanisms, which directly convert mechanical stimuli into quantifiable electrical signals. Unlike generic conductive networks, these mechanisms must be

strategically designed to target specific types of mechanical inputs such as pressure, strain, or bending. For instance, volume transition-type systems rely on structural changes in the hydrogel matrix under stress, altering ion mobility or local concentration to produce resistance or capacitance shifts [76]. This mechanism offers high sensitivity to osmotic or swelling-induced pressures but is often limited in response speed due to the relatively slow diffusion of water and ions through the polymer network. In conductive network reconfiguration, mechanical deformation modulates inter-filler contact resistance or tunneling distances, enabling highly sensitive piezoresistive responses [95]. While this approach achieves rapid signal output and high gauge factors, its stability can be compromised by filler re-aggregation or detachment under large or cyclic deformation, leading to signal drift. Alternatively, ion migration mechanisms exploit the movement of charged species within the hydrogel under strain, generating ion-based potentials or conductivity variations that mimic biological signal transduction [96]. Ionic sensors excel in mimicking biological signal transmission and often exhibit good linearity and self-recovery, yet their sensitivity may be lower compared to percolation-based systems, and their performance can be significantly influenced by environmental humidity and ion concentration. The choice of mechanism inherently involves trade-offs between sensitivity, response speed, stability, and fabrication complexity, necessitating alignment with the intended sensor application and operational environment.

## 4.2 Improvement of 3D Printing Process Parameters

The transition from material design to functional device integration is realized through 3D printing. Unlike conventional fabrication methods, 3D printing empowers the precise creation of three-dimensional hydrogel structures, where the printing process itself dictates the final geometry, porosity, and feature resolution. This section critically examines the key correlations between the control of printing parameters, the resulting printed structures, and the final sensing performance in prevalent 3D printing technologies.

### 4.2.1 Material Parameters

Several key material parameters will influence overall structural integrity and functional performance: ink viscosity, solid content, crosslinking density, and shear-thinning index. The viscoelastic modulus of hydrogels is a key indicator for evaluating their viscoelastic properties, primarily comprising the storage modulus ( $G'$ ) and the loss modulus ( $G''$ ) [97].  $G'$  is also referred to as the elastic modulus, which denotes the energy storage capacity of a material during reversible elastic deformation, and characterizes the elastic property of the material.  $G''$  is also known as the viscous modulus, representing the energy dissipated during irreversible deformation of the material and reflecting the magnitude of its viscosity. The ratio of the loss modulus  $G''$  to the storage modulus  $G'$  is referred to as the loss tangent, reflecting the viscoelastic proportion of the material. Factors such as crosslinking density, polymer chain length and rigidity, solvent nature, and temperature all influence this modulus ratio [98, 99].

Moreover, the viscoelastic modulus governs the feasibility of 3D printing. A hydrogel with an appropriate viscoelastic modulus ensures sufficient fluidity to pass smoothly through a nozzle or extruder while retaining adequate shape fidelity so that it does not excessively deform or collapse after deposition. If the modulus is too low, the hydrogel will be unable to maintain its shape, and the desired architecture cannot be formed; if it is too high, the printing equipment may be unable to drive the material forward, leading to nozzle clogging and other issues that hinder successful printing [97]. Achieving this balance, therefore, represents a key step in addressing the intrinsic challenge of reconciling printability with functional performance in hydrogel-based sensor fabrication.

In the material design of 3D printed hydrogels, the precise matching of solid content and crosslinking density is the core principle for achieving performance customization. Solid content refers to the total proportion of non-volatile components in the ink precursor. It primarily determines the ink's viscosity, thereby influencing its rheological behavior and printability. Upon gelation, solid content directly correlates with the hydrogel's mechanical strength and swelling stability. Generally, a higher solid content means a greater number of polymer chains or fibers per unit volume to bear the load, significantly enhancing the material's compressive modulus and tensile strength [100]. Concurrently, the inherently dense initial structure associated with high solid content effectively restricts the osmotic driving force of water molecules, resulting in a lower equilibrium swelling ratio, which is vital for maintaining the geometric accuracy of the printed structure.

Crosslinking density refers to the number of crosslinking points per unit volume [100]. Therefore, increasing the crosslinking density is one of the most effective ways to enhance hydrogel stiffness. However, this gain in stiffness often comes at the cost of reduced ductility and toughness. A density that is too low results in overly soft and structurally unstable materials, whereas excessive density leads to brittleness and loss of flexibility. Ultimately, device performance is not determined by a single parameter but arises from the complex coupling between solid content and crosslinking density. Together, they determine the density of the hydrogel network. Solid content provides the physical load-bearing matrix and entanglement points, while crosslinking density contributes chemical elastic restorative force. This coupling results in characteristic synergistic and trade-off effects.

Shear-thinning is a core rheological property of hydrogel inks. When subjected to shear stress, the viscosity of hydrogel inks significantly decreases, facilitating easier flow. Once the shear stress is removed, the ink rapidly regains its higher viscosity, thereby maintaining the shape and structural stability of the deposited material. This property directly addresses the challenge of achieving high structural fidelity while maintaining printability, as it allows the ink to flow during extrusion and then retain its shape after deposition [101]. In fact, the intrinsic properties of the polymer have a significant impact on the shear-thinning behavior of the ink. The core of regulating the shear-thinning behavior of hydrogel inks lies in their internal reversible physical cross-linking networks. By adjusting polymer parameters (concentration, molecular weight, chain rigidity) or introducing interactive additives (dynamic

cross-linkers, nanofillers), the strength of the network structure and the kinetics of its dissociation and reformation can be controlled [102].

In addition to the composition and structure within the polymer, the elasticity of the fluid, temperature, and pH value can also significantly affect its shear-thinning properties [99]. Moreover, external conditions such as shear stress and shear rate also have a direct impact on shear-thinning behavior. An increase in shear stress and shear rate can disrupt the internal structure of the fluid, resulting in a decrease in viscosity and an enhanced shear-thinning effect. The composition of the fluid and the presence of additives play a significant role. The nature of the solvent and additives (such as inorganic fillers, plasticizers, etc.) can alter the structure of the fluid and the intermolecular interactions, thereby modulating its shear-thinning characteristics [101, 103, 104]. These factors interact with each other to collectively determine the shear-thinning behavior of hydrogel inks.

#### 4.2.2 3D Printing Parameters

Printing precision is one of the key factors affecting the quality of 3D printed products. Core parameters during the printing process, such as extrusion rate, nozzle diameter, printing layer height, printhead moving speed, and photocuring energy/exposure time, directly affect the microstructure of the material, which in turn determines the performance of the entire device.

As a core component of 3D printers, nozzle selection directly governs print quality, speed, and material compatibility, making an appropriate choice essential to meet specific printing needs and application scenarios. Generally, smaller nozzles enable higher-resolution prints with finer details, yet at reduced speeds. Conversely, larger nozzles enhance printing throughput but often compromise precision. When selecting the nozzle size, a trade-off should be made based on the specific project requirements. If both precision and speed need to be considered, variable-diameter nozzles or adjusted printing parameters can be used to optimize the printing effect. By introducing the concept of adaptive nozzle 3D printing (AN3DP), the nozzle diameter and cross-sectional shape can be dynamically changed during the printing process. The AN3DP nozzle consists of eight independently controllable muscle-driven pins, which are arranged around a flexible and pressure-resistant membrane. This design adopts a cone angle optimized for extruding shear-thinning inks and a pointed tip suitable for confined-space printing (such as conformal printing and embedded printing). Compared with traditional 3D printing methods, the efficacy of AN3DP is demonstrated by fabricating components with continuous gradients, which eliminates the need for discretization and achieves higher density and contour precision [105].

Since 3D printing builds objects through layer-by-layer deposition, layer thickness significantly affects the surface roughness of printed parts [95, 106]. A larger nozzle diameter combined with a thicker layer increases printing speed but yields a rougher surface, whereas a smaller nozzle with a thinner layer improves precision at the cost of slower printing. Therefore, nozzle size and layer thickness must be selected judiciously according to the model geometry and intended application. Additionally, successful printing relies on the

synchronized coordination between printing speed and extrusion rate [107, 108]. If the printing speed excessively outpaces extrusion, inadequate material deposition and filament breakage may occur. Conversely, if extrusion exceeds printing speed, material accumulation and uneven distribution result. Thus, printing speed must be carefully tuned, with distinct settings for contours, infill, and support structures. Typically, a reduced speed is recommended for the first layer to enhance bed adhesion and overall print quality. Moreover, Printing temperature encompasses both the extruder nozzle temperature and the heated bed temperature. The extruder temperature primarily governs material bonding, layer adhesion, and filament flow behavior [99]. Excessively low temperatures can lead to poor bed adhesion, interlayer delamination, and nozzle clogging, while overly high temperatures may cause the extruded material to behave like an unmanageable fluid rather than a coherent filament. Both the nozzle and bed temperatures are critical parameters that require real-time monitoring and dynamic adjustment throughout the printing process.

In 3D photocuring printing, photocuring energy, exposure time, and photo-initiator are three key parameters. They are interrelated and crucial to the printing effect [109]. In UV curing, sufficient energy density is the fundamental guarantee for ensuring deep-layer curing and meeting the required material performance. It is jointly determined by irradiance ( $I$ ) and exposure time ( $t$ ), following the formula: Energy ( $E$ ) = Irradiance ( $I$ ) $\times$ Time ( $t$ ). Exposure time directly controls the accumulation process of light energy. A longer exposure time means more light energy input, which not only ensures the curing depth but also affects the integrity of the cross-linked network. As a comprehensive reflection of exposure time and light intensity, photocuring energy must meet two basic requirements: first, reaching the critical energy for initiating polymerization; second, ensuring that the energy can fully penetrate to the preset curing depth [48].

The photocuring of hydrogels relies on photoinitiators that absorb photons and generate active free radicals to initiate polymerization. The absorption profile and reaction efficiency of the photoinitiator define the energy threshold required for resin curing [110]. When its absorption wavelength aligns with the light source and exhibits high efficiency, sufficient curing can be achieved with lower energy input. Selecting an appropriate photoinitiator requires consideration of its absorption range, application context, and cytotoxicity. For instance, Irgacure 2959 (250–330 nm) suits acellular systems but shows moderate to high cytotoxicity and requires post-processing. TPO (350–420 nm) enables deep curing in thick or cell-laden constructs with low cytotoxicity. LAP/NAP (365–405 nm) is well-suited for cell encapsulation and 3D bioprinting due to its low cytotoxicity. These distinct characteristics allow for tailored photoinitiator selection according to specific photocuring applications. Meanwhile, there remains an unavoidable contradiction between energy consumption and efficiency: photocuring requires a high-intensity UV light source, while thermal curing relies on an oven or laser, resulting in energy consumption that is several orders of magnitude higher than that of traditional injection molding. In recent years, research has shifted toward the self-powered curing pathway. Existing studies have proposed an

integrated strategy of frontal polymerization-3D printing-in-situ curing, and designed printable inks composed of Carboxer 940, acrylamide/acrylic acid, and a TEMPO inhibitor. This enables instant triggering and self-propagating curing within seconds, resulting in a sharp reduction in energy consumption and strong interlayer bonding, successfully printing complex soft gels with high fidelity. This provides a universal new approach for energy-efficient additive manufacturing of soft materials [111].

In addition to light intensity, attention should also be paid to the effect of oxygen inhibition. Oxygen competitively consumes free radicals, leading to poor curing of hydrogels, which is manifested as sticky and limp gels with low strength. In conclusion, in 3D photocuring printing, energy and exposure time need to be comprehensively adjusted based on factors such as resin properties, light source wavelength, and ambient temperature. Through testing and practice, identifying the optimal parameter combination suitable for specific materials and application scenarios is the key to ensuring printing quality and efficiency.

#### 4.2.3 Post-Processing

3D printing technology has successfully endowed hydrogels with pre-designed macroscopic geometries. However, for their necessary mechanical properties, structural stability, and biological activity as functional devices, a sophisticated post-processing procedure is also an essential step. Through a series of physical or chemical methods, the metastable polymer network formed in the initial printing stage is actively guided and reconstructed, thereby achieving the improvement of the final properties of hydrogels. Various post-processing methods, including chemical crosslinking, freeze-thaw, drying annealing, salting-out, and alkali treatment, are commonly employed [112].

Crosslinking treatment is a fundamental strategy for constructing stable three-dimensional networks, serving as the structural foundation for hydrogel devices. Chemical crosslinking establishes a permanent network through covalent bonds, achieved by using agents (e.g., glutaraldehyde and genipin) or by activating residual reactive groups via light or heat. This approach significantly enhances the elastic modulus and tensile strength of the material while effectively suppressing excessive swelling in aqueous environments, thereby ensuring long-term dimensional stability and mechanical reliability of the device [113]. Physical crosslinking, utilizing ionic bonds, hydrogen bonds, or host-guest interactions, offers a dynamic and reversible network formation strategy. While generally providing lower mechanical strength than chemical crosslinking, such non-covalent bonds confer hydrogels with notable self-healing ability, injectability, and environmental responsiveness to pH or temperature. This addresses key challenges in interfacial repair and adaptability within dynamic biological settings, paving the way for intelligent bio-inspired devices. Freeze-thaw cycling represents a distinct form of physical crosslinking, particularly effective for crystalline polymers like polyvinyl alcohol (PVA). Through iterative freezing and thawing, polymer chains align within ice-crystal templates, forming microcrystalline domains that serve as robust physical crosslinks. This process

significantly enhances the mechanical properties of hydrogels, enabling them to retain high water content while achieving toughness and wear resistance comparable to natural cartilage tissue.

To enable the application of hydrogels in specific scenarios, drying treatment is another type of critical post-processing technique. Although conventional atmospheric-pressure drying or heat drying is simple to operate, it is difficult to avoid network collapse caused by capillary forces. In contrast, freeze-drying technology can almost perfectly preserve the 3D porous structure constructed by printing by directly sublimating the ice crystals in the sample, ultimately obtaining hydrogel aerogels with a high specific surface area. Such materials show great potential in fields such as tissue engineering scaffolds, supercapacitors, and adsorption separation [114].

To avoid the potential biotoxicity of chemical crosslinking agents and further enhance the performance of physical hydrogels, physical post-processing methods such as drying, annealing, and salting-out/alkali treatment have been developed. Drying annealing combines the close segment contact caused by dehydration and the segment mobility provided by heat treatment, thereby inducing the formation of more and more stable physical crosslinking points (e.g., hydrogen bonds). Ultimately, this significantly improves the mechanical properties of the hydrogel after rehydration [115]. In contrast, salting-out and alkali treatment involve placing the hydrogel in a specific solution environment. This effectively weakens the interaction between the polymer and water, drives phase separation and tight aggregation of polymer chains, and further forms a dense network dominated by strong hydrogen bonds and hydrophobic interactions. This not only achieves a leap-forward increase in the hydrogel's modulus and strength but also effectively controls its swelling behavior [112].

## 5 Application of 3D-Printed Hydrogel Flexible Sensing Devices

### 5.1 Wearable Health Monitoring

In recent years, wearable electronics have ushered in unprecedented opportunities for continuous health monitoring. Hydrogel-based electronic technologies, distinguished by intrinsic biomimicry in combination with appreciable electrical conductivity, have emerged as compelling alternatives to conventional metallic electrodes at biotic-abiotic interfaces. Against this backdrop, 3D-printed hydrogels have become a key technology. Compared with traditional manufacturing methods, 3D printing offers advantages of high precision and customization, enabling the creation of patient-specific structures with complex geometries and specific mechanical properties. Liu et al. developed a PEDOT: PSS-based bioink whose rheological and cross-linking characteristics permit high-fidelity 3D printing [116]. The as-printed bioelectronics exhibit mechanical and electrical properties that closely match those of native tissues, establishing robust electroactive interfaces with *in vivo* biological tissues/organs.

Although hydrogels can effectively mimic the mechanical behavior of native tissues, achieving both mechanical

robustness and high electrical conductivity remains a significant challenge. Based on projection microstereolithography (PμSL) technology, Wang et al. introduced hydrophilic trihydric alcohol as a benign solvent for the photoinitiator TPO-L, utilized nano-hydroxyapatite (nHAp) to enhance stretchability, and integrated high-concentration ionic salts and trihydric alcohol as conductive media and antifreeze agents. Consequently, the developed hydrogel system exhibits excellent mechanical properties (> 2500% elongation), electrical conductivity, and anti-freezing performance (around  $-115^{\circ}\text{C}$ ) (Figure 6(a)). It can serve as a flexible strain sensor for real-time monitoring of human motions and weak physiological signals (Figure 6(b)), and further function as a brain-computer interface (BCI) to accurately acquire electroencephalographic (EEG) signals from the brain, including alpha ( $\alpha$ ) and beta ( $\beta$ ) waves that reflect the overall information of brain activities (Figure 6(c)) [117]. The hydrogel proposed in this study holds promising application prospects in electronic skin, human-machine interaction, and even wearable devices operating under extremely low-temperature conditions. In the future, the integration of microscale 3D printing technology will enable the rapid fabrication of multifunctional flexible electronics with complex 3D structures and sophisticated brain-computer interfaces.

Current hydrogel-based epidermal electronics often face constraints in achieving integrated multifunctionality, such as concurrent physiological monitoring and energy autonomy. To address this, recent research has focused on co-designing material compositions and device architectures that combine sensing, energy harvesting, and stimuli-responsive behaviors within a single, printable hydrogel system. Yuan et al. developed a 3D-printable multifunctional hydrogel that can be precisely fabricated into lattice or hollow architectures [118]. This wearable device enables high-fidelity multiplexed physiological monitoring (e.g., joint movement, swallowing, and EMG) and integrates a paper-based TENG for *in-situ* energy harvesting ( $83 \text{ mW} \cdot \text{m}^{-2}$ ), establishing a self-powered, closed-loop health management system. In parallel, Weng et al. developed a sandwich-structured, self-powered hydrogel that can be 3D-printed into arbitrary soft sensors [119]. This battery-free platform intrinsically distinguishes multiple mechanical stimuli (stretching, bending, etc.) and enables contactless gesture recognition, facilitating applications in unobtrusive health monitoring and seamless human-machine interaction.

Driven by the burgeoning demand for wearable electronics, contemporary research is converging on the simultaneous realization of high electrical conductivity, superior mechanical robustness, and intrinsic biological functionalities (e.g., antimicrobial activity, biocompatibility) while maintaining precision printability and environmental sustainability. Martinez et al. presents a gut-on-a-chip system based on DLP-SLA 3D bioprinting, utilizing PEGDA-GelMA composite hydrogel as the bioink to fabricate perfusable channels with villus-like structures (Figure 6(d)) [120]. It enables the co-culture of stromal compartments embedded with fibroblasts and intestinal epithelial cells, recapitulating the 3D compartmentalized structure of the intestinal mucosa (Figure 6(e)). Integrated with coplanar electrodes, the chip

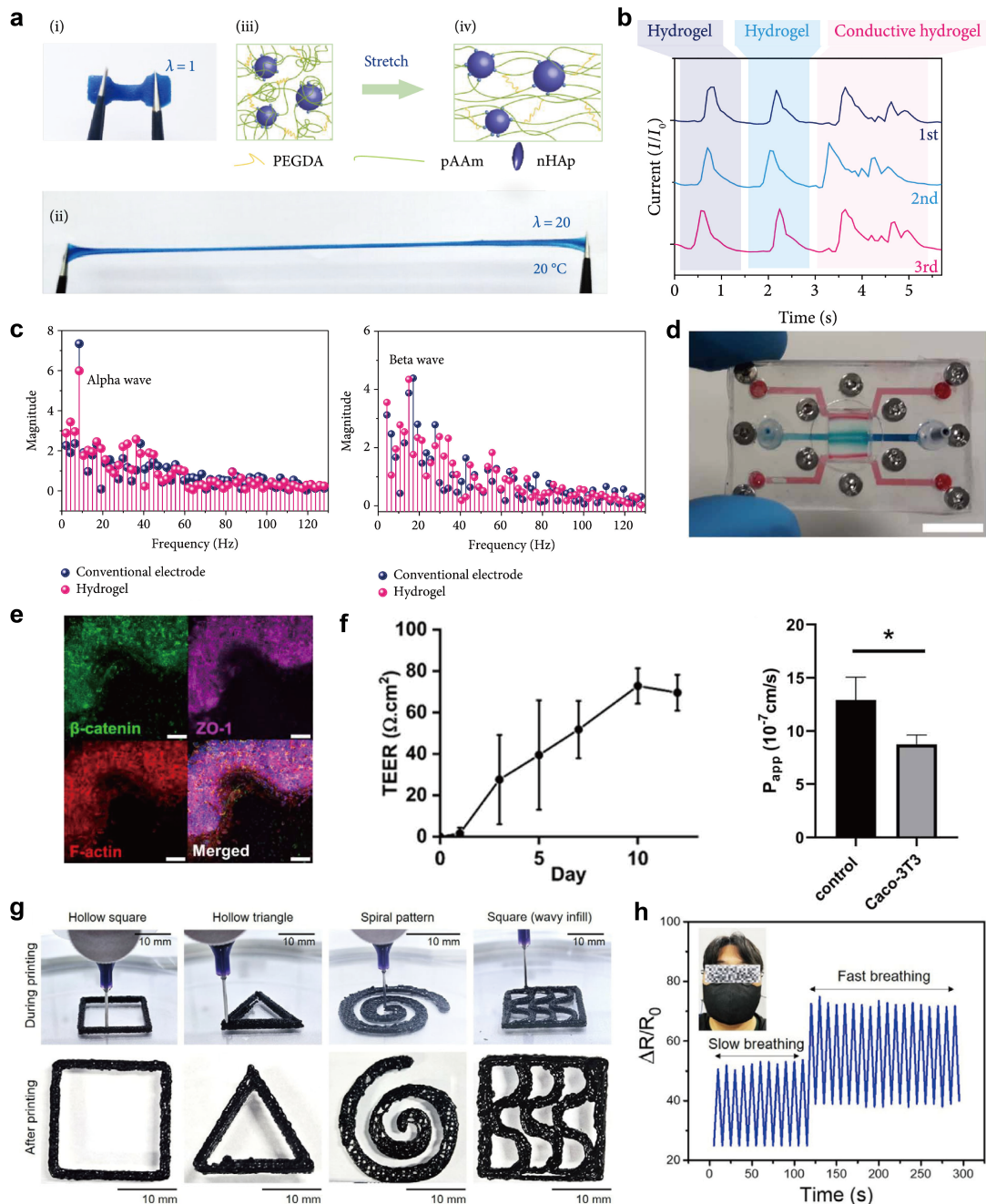


**Figure 6:** Representative examples of 3D-printed hydrogel sensors applied in wearable health monitoring. (a) 2500% ultra-elongation via nHAp-polymer interactions, ensuring robust mechanical performance for wearable use [117]. (b) Real-time current responses of throat-attached sensor to pronouncing target phrases. Exhibits high sensitivity and repeatability, enabling accurate detection of weak physiological signals [117]. (c) Fourier transforms of EEG signals showing 8 Hz alpha wave (eyes closed) and beta wave (eyes open). Validates precise brain signal capture comparable to conventional electrodes, enabling reliable brain-computer interface applications [117]. (d) Top view of the tri-channel microfluidic chip with encapsulated hydrogel. Enables stable perfusion and reliable integration for dynamic co-culture [120]. (e) Confocal projection of villi-like hydrogel with junction markers. Confirms intact epithelial barrier formation, mimicking in vivo mucosa structure [120]. (f) Combined Papp and TEER plots. Shows low permeability and in vivo-like TEER, verifying robust barrier function and real-time monitoring capability [120]. (g) Printability assessment of a PVA/gelatin/CNT/CNC ink (PVG/N2C1) using complex 2D patterns, confirming its high resolution and structural fidelity [122]. (h) Real-time respiratory monitoring using the PVG/N2C1 E-skin patch, showcasing its function as a multimodal sensor for physiological signals [122].

achieves real-time monitoring of transepithelial electrical resistance (TEER) via electrochemical impedance spectroscopy while supporting optical observation. The formed epithelial barrier exhibits low permeability and TEER values close to *in vivo* levels, providing a fully functional *in vitro* model for intestinal physiological and pathological research as well as drug screening (Figure 6(f)). Yu et al. developed a PVA-based hydrogel ink that rapidly solidifies during low-temperature extrusion, enabling high-precision 3D printing of sophisticated structures with well-preserved, pre-defined microstructures, such as intricate Chinese-knot motifs [121]. Kim et al. developed a mucus-like E-skin from a PVA/gelatin/CN-T/CNC hydrogel. The synergistic effect of CNTs and CNCs enabled high-resolution 3D printing (Figure 6(g)), yielding a patch with extraordinary stretchability ( $\sim 1000\%$ ), conductivity ( $\sim 5 \text{ S} \cdot \text{m}^{-1}$ ), and multimodal sensing capabilities for motion, temperature, and humidity (Figure 6(h)). It also features strong bio-adhesion, NIR-responsive antibacterial function for wound treatment, and good cytocompatibility [122].

## 5.2 Motion Detection

The integration of 3D printing with functional hydrogels has greatly advanced the development of flexible sensors for human motion detection. Recent research has increasingly focused on strategies such as multi-material compositing and microstructural engineering to capture a wide range of biomechanical signals effectively. To address the trade-off between mechanical robustness and sensitivity, Huang et al. developed a DLP 3D-printed flexible hydrogel sensor with a conic-pyramid multilevel microstructure (Figure 7(a)) [123]. Using an AM-PEGDA double network as the matrix, a  $\text{Mg}^{2+}/\text{Na}^+$  dual-ion system for conduction, and 30 wt% glycerol for moisture retention, the sensor achieves a high sensitivity of  $0.544 \text{ Kpa}^{-1}$  (0–0.8 Kpa), a response time of 30 ms, and signal attenuation  $< 4\%$  after 10,000 cycles. It enables real-time monitoring of finger/wrist bending motions (Figure 7(b)) and is suitable for high-performance wearable motion sensing. Wu et al. developed a DLP 3D-printable silk fibroin hydrogel with a hybrid cross-linked network, providing tunable mechanics, strong yet reversible skin adhesion, and enhanced water retention [124]. The material served as a reliable strain sensor for detecting various body movements. By fabricating a 10-channel sensor array, the system achieved 97.5% accuracy in hand gesture recognition using machine learning, demonstrating a comfortable and effective approach to long-term wearable human-machine interfaces (Figure 7(c–d)).

Zheng et al. employed DIW 3D printing to fabricate NMAL (natural, multifunctional, adaptive, and living) hydrogels [118]. The sensor responded to strain ( $\text{GF} \approx 2.5$ , 400% strain), temperature, and pH ( $-13.68 \text{ mV/pH}$ ), retained over 200% resistance change after 1000 cycles at 100% strain, and could function as a TENG ( $1.2 \mu\text{W}$ , 40 N). It detected motion of the jaw, throat, and multiple joints, supporting applications in smart fitness and daily health management (Figure 7(e)). Tang et al. created a self-powered soft sensor using an innovative 3D printed galvanic cell design that requires no external power [119]. The device effectively monitors various body movements, including arm bending

and breathing rhythms, by generating distinct electrical signals in response to mechanical stimuli such as stretching, bending, and pressing. This technology provides a versatile platform for autonomous health monitoring and human-machine interaction applications. These studies illustrate how integrated material and energy-autonomous designs are advancing toward maintenance-free, intelligent sensing systems for motion monitoring and human-machine interaction.

Zhang et al. prepared polyacrylamide hydrogel sensors via DLP 3D printing using MXene/SDS as conductive fillers and biomimetic microneedle arrays (pyramid/cone/cylinder) as microstructures [125]. The pyramid-structured sensor exhibited the highest sensitivity ( $\text{GF} = 7.74$  at  $100 \mu\text{m}$  thickness), detecting micro-displacements as small as  $20 \mu\text{m}$ . It enabled accurate tracking of knee joint flexion ( $0^\circ$ – $135^\circ$ ), torsion ( $5^\circ$ – $20^\circ$ ), and lateral sliding ( $40$ – $200 \mu\text{m}$ ) (Figure 7(f–g)). The sensor also showed over 99% antibacterial activity and  $> 85\%$  HaCaT cell viability, supporting its potential in clinical knee rehabilitation and early osteoarthritis monitoring. In a related approach, Nezafati et al. developed a self-healing conductive hydrogel via UV-triggered 3D printing, integrating carbon nanotubes and polydopamine within a dual-network structure [125]. This sensor exhibited high sensitivity ( $\text{GF} \approx 10.97$ ), rapid response (120 ms), and efficient self-recovery, while also demonstrating strong antibacterial activity. Its functionality was further validated through wireless monitoring of multiple joint movements and physiological vibrations, highlighting its suitability for interactive and remote rehabilitation applications.

The perfect combination of high-performance sensing and biocompatibility not only enables full-scale monitoring capabilities that cover macroscopic limb movements to microscopic physiological vibrations, but also opens up new pathways for telemedicine and Human-machine interaction through wireless design. Notably, these technologies can meet clinical-grade monitoring accuracy while possessing durability for daily use. This marks the evolution of wearable devices from auxiliary tools to professional medical equipment and lays a technical foundation for building digital health management systems.

## 5.3 Human-Machine Interaction and Robotics

Human-machine interfaces (HMIs) aim to establish a seamless, bidirectional communication channel between the human body and external devices. The unique combination of softness, biocompatibility, and customizable manufacturing offered by 3D printed hydrogels positions them as an ideal material platform for next-generation HMIs, which are transitioning from rigid, obtrusive systems to comfortable, wearable, and even implantable forms. Inspired by natural hierarchical composite design principles, Zhai et al. proposed a hierarchical fabrication strategy for ceramic-reinforced organo-hydrogels [126]. Through direct ink writing (DIW) 3D printing, this strategy achieves the aligned arrangement of ceramic platelets, reinforces the polyvinyl alcohol (PVA) matrix via solution substitution, and optimizes the interface bonding through silane treatment. Furthermore, bioinspired macro-architectures such as unidirectionally aligned, Bouligand, and

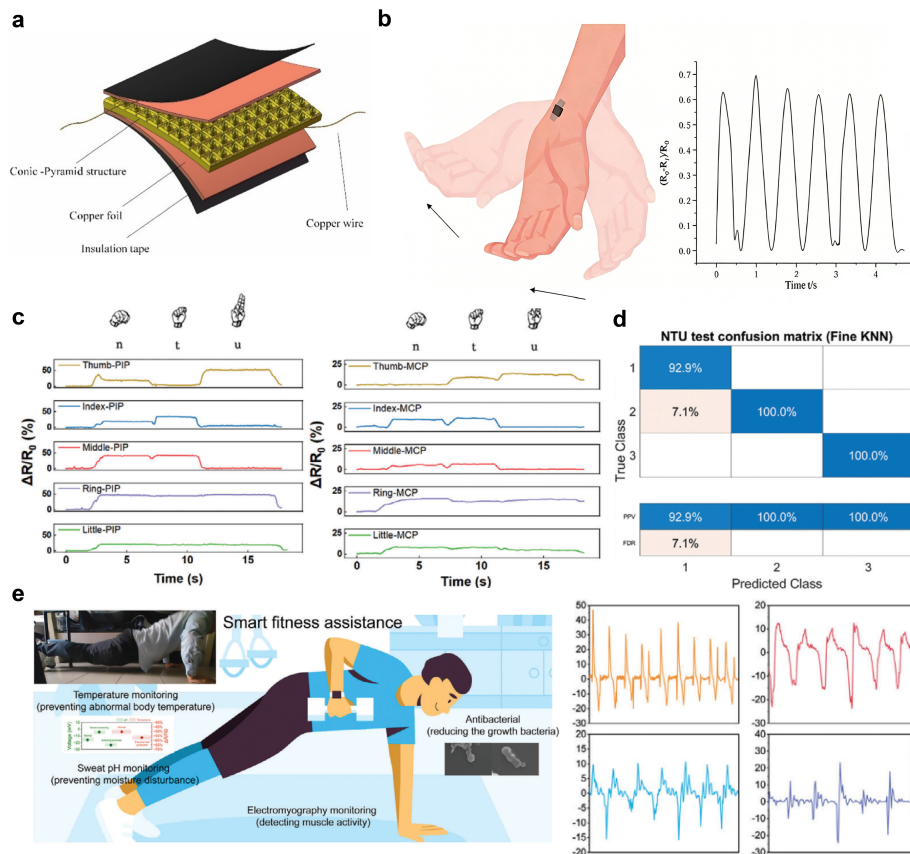


**Figure 7:** 3D-printed hydrogel sensors with tailored microstructures and self-powering functionality for monitoring human motion and biomechanical signals. (a) Schematic of the conic-pyramid hydrogel sensor. Shows integrated structure with electrodes, ensuring stable signal transmission and mechanical robustness for wearable use [123]. (b) Resistance signals during wrist bending, enabling sensitive real-time monitoring of large-joint motions [123]. (c) Resistance changes corresponding to specific sign language gestures (N, T, U), demonstrating the sensor’s capability for motion capture. (d) Confusion matrix from the classification of sign language gestures, highlighting the accuracy enabled by combining sensor data with machine learning [124]. (e) Conceptual diagram of a natural, multifunctional, adaptive, and living (NMAL) hydrogel system for capturing exercise-induced electrophysiological signals. (f) Working principle of a biomimetic microneedle-based sensor for detecting micro-displacements [118]. (g) Sensor signals during simulated knee lateral slip, demonstrating its ability to monitor complex joint kinematics for rehabilitation and early warning [118].

crossed lamellar structures are printed (Figure 8(a)). The resulting material exhibits a combination of high stiffness (up to 9.6 MPa), high strength (up to 7.8 MPa), and excellent toughness (fracture energy reaching 31.1 kJ/m<sup>2</sup>), along with good electrical conductivity (up to 8.8 S/m), wide temperature tolerance (stable operation from −30 to 60 °C), and long-term environmental stability. Successfully integrated into a multifunctional smart sensing glove, it enables multi-mode human-machine interaction applications including touch screen interaction and robot control (Figure 8(b)), providing an efficient design paradigm for 3D printed hydrogels in mechanically demanding flexible electronics fields.

He et al. developed 3D-printable ionogels via photopolymerization-induced microphase separation that overcome the key limitations of conventional human-machine interfaces [47]. These materials maintain high conductivity and sensitivity (15.1 kPa<sup>−1</sup>) across an extreme temperature range, enabling reliable pressure sensing in robotic grippers and breaking the traditional trade-off between performance and environmental adaptability for industrial HMI applications (Figure 8(c–d)). Tang et al. developed a self-powered soft sensor using a 3D printed galvanic cell structure, which

functions without an external power source [119]. It exhibits dual sensitivity to pressure (195 μA/N) and temperature (4.5 μA/°C), and can be applied in human motion monitoring, contactless gesture recognition, and object size identification. This work effectively addresses the power dependency of conventional HMIs, enabling applications in scenarios such as outdoor rescue robotics.

Li et al. developed a flexible ionoelectronic tactile sensor based on freeze-printed PEDOT: PSS-PVA hydrogel grids (Figure 8(e)) [127]. The sensor exhibits an excellent linear response ( $R^2 = 0.993$ ) over a wide pressure range of 0–220 kPa, along with tissue-level compliance (elastic modulus: 127–404 kPa) and linear compression properties. As a wearable human-machine interface, it reduces waveform tracking errors by 47.6%–64.1% in robotic teleoperation; as a robotic fingertip sensor (Figure 8(f)), it can detect soft tissue elasticity under biocompatible pressure (average error: 8.9%), successfully resolving the traditional trade-off between wide sensing range and high precision.

Yang et al. developed a frost-resistant lignin-based hydrogel via 3D printing that retains flexibility and sensing function

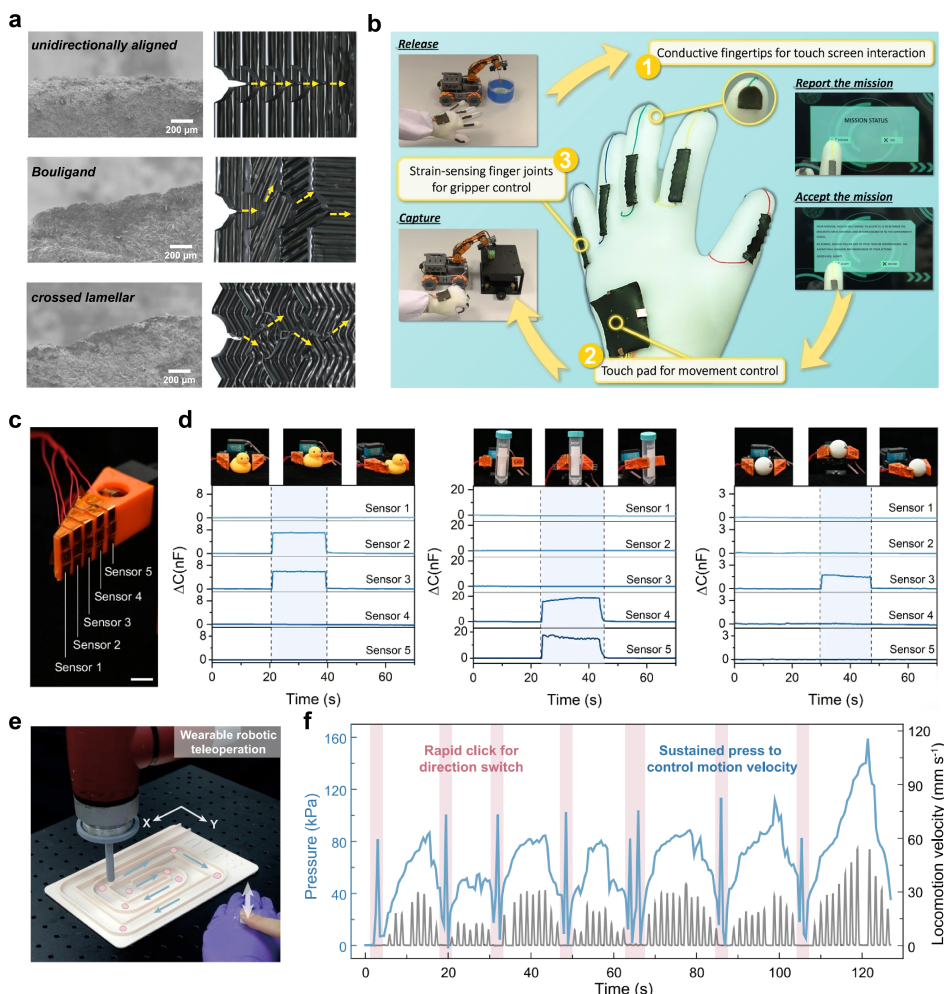


**Figure 8:** 3D-printed hydrogel-based interfaces enabling programmable human-machine interaction and enhanced robotic tactile sensing. a) By regulating crack propagation paths through the biomimetic structural designs of unidirectional alignment, Bouligand, and cross-lamellar architectures, the mechanical durability of 3D-printed hydrogel devices is enhanced [126]. b) A multifunctional smart sensing glove based on multi-biomimetic architectures composite organohydrogel and its human-machine interaction applications [126]. (c) Robotic hand integrated with an array of five ionogel-based capacitive sensors, providing tactile feedback for object manipulation [47]. (d) Real-time capacitance signals from the sensor array during robotic grasping and release of various objects, demonstrating robust and sensitive pressure detection [47]. (e) Wearable interface for robotic teleoperation via pressure input [127]. (f) Correlation between the pressure detected by a 3D lattice sensor and robotic velocity during a targeted task, validating its precision for closed-loop control [127].

at  $-40^{\circ}\text{C}$ , enabling reliable HIMs in extremely low temperature environments such as polar and industrial settings [128]. Lai et al. fabricated a polyionic glycerol hydrogel with a semi-interpenetrating network using 3D printing, exhibiting low contact impedance and strong skin adhesion [129]. When configured as a high-density sEMG electrode array and combined with a CNN algorithm, the system achieved accurate recognition of 26 hand gestures and responsive prosthetic control, advancing electromyography-based HMIs for precision prosthetic applications.

The precise design of functional materials and innovative integration of system architectures together point toward the development direction of next-generation human-machine interaction systems. Advanced 3D printing technology is used to fabricate devices, enabling leapfrog progress in the environmental adaptability and energy autonomy of sensing terminals. This confirms the unique advantages of additive manufacturing in constructing complex functional structures,

opens up an important path for developing high-performance embedded sensing systems, and provides a new technical paradigm for complex scenarios such as industrial automation and outdoor rescue. The recent examples from the last five years have been summarized in Table 2.

## 6 Conclusions and Prospects

As a key interface linking the physical and biological worlds, flexible mechanical sensors have evolved continuously through innovations in materials and processes, progressing from early rigid metallic structures to a new generation of sensing platforms based on flexible polymers. Among these, hydrogels are emerging as a core material carrier in flexible sensing due to their mechanical properties that closely match human soft tissues, excellent biocompatibility, and tunable functionality. Concurrently, 3D printing technology, leveraging its unique capabilities in on-demand shaping and

**Table 2:** Characteristics of recently reported 3D-printed hydrogel sensors

Hydrogel	3D Printing Techniqu	Sensor Mechanism	Sensitivity	Strain Range	Durability (cycles)	Application	Ref.
ALG/AM	DIW	Resistive	1.2	0–1000%	200	Flexible Electronics and Smart Devices	[130]
PEDOT:PSS/PVA/PAA-NHS	DIW	Resistive	N/A	N/A	5000	Flexible Electronics and Smart Devices	[116]
PEDOT:PSS/HPU	DIW	Resistive	N/A	N/A	5000	Wearable Health Monitoring	[87]
PVA/CS/P(NIPAM-co-AM)	DIW	Triboelectric	2.5	0–400%	1000	Flexible Electronics and Smart Devices	[118]
PAA/PDA/Cu/Cu <sup>2+</sup> DLP, DIW/MnO <sub>2</sub>		Galvanic cell self-powering	N/A	N/A	3600	Human-Machine Interaction and Robotics	[119]
SF/AAM/ChCl	DIW	Resistive	5.33 1.25 kPa <sup>-1</sup>	0–73.38% < 7 kPa	1000	Wearable Health Monitoring	[131]
PVA/TA/PANI@BC	DIW	Resistive	3	10–200%	200	Wearable Health Monitoring	[121]
PVA/Gel/CNT/CNC	DIW	Resistive	6.5	0–250%	500	Flexible Electronics and Smart Devices	[122]
PAMPS/PAAc	DIW	Resistive	0.253	350–460% < 5 kPa	600	Wearable Health Monitoring	[63]
SF/PAAm/PAAc	DLP	Resistive, Capacitive	1.29	0–100%	80	Wearable Health Monitoring	[124]
AHEC/OGG-PDA/ZnZn <sup>2+</sup> /MWCNTs-SH	DIW	Resistive	10.97	58–80%	1000	Wearable Health Monitoring	[132]
PAM/MXene/SDS	DLP	Resistive	N/A	N/A	100	Wearable Health Monitoring	[125]
AAm/PEGDMA	DLP	Resistive Capacitive	1.54	200–400%	N/A	Wearable Health Monitoring	[133]
BA/PEGMA	DLP	Capacitive	15.1 kPa <sup>-1</sup>	< 12 kPa	1000	Wearable Health Monitoring	[47]
LIG/ACMO/DMAEA-Q	DLP	Resistive	1.94 1.68	200–350% 0–50%	10000	Wearable Health Monitoring	[128]
PNaSS/PDMAEA-Q	DIW	Capacitive	N/A	N/A	N/A	Human-Machine Interaction and Robotics	[129]
PEDOT:PSS/PVA	DIW	Capacitive	0.022 ± 0.002 kPa <sup>-1</sup>	< 220 kPa	4000	Human-Machine Interaction and Robotics	[127]

precise customization, provides an innovative manufacturing pathway for the structural design and functional integration of hydrogel sensors.

This review systematically summarizes advances in the field. It begins by explaining the operating principles of various sensors and the material selection underlying their performance. It then analyzes the characteristics and suitable applications of different printing techniques applicable

to hydrogel additive manufacturing. This is followed by an in-depth discussion of ink design principles that influence printability and device performance. Finally, the review outlines the current state of research on 3D-printed composite hydrogel sensors and prospects for future development. Although significant progress has been made, several critical directions remain to be explored to fully realize the potential of 3D-printed hydrogel sensors, as illustrated in [Figure 9](#).

## 6.1 New Materials and Processes from Intelligent Design to Bio-Integration

Currently, most composite material systems rely on physical blending. The weak physical adsorption and mechanical interlocking between their components easily lead to unstable dispersion of functional units and phase separation/aggregation. Additionally, the poor interfacial compatibility of components restricts the efficiency of stress transfer and charge migration, resulting in uneven material performance and insufficient synergistic effects. In the future, hydrogel materials need to shift from physical stacking to intrinsic function integration driven by dynamic bonds. The core lies in using dynamic covalent bonds or highly directional supramolecular interactions. During the material synthesis stage, pre-designed conductive units, self-healing modules, etc are covalently woven into a unified and homogeneous three-dimensional network through in-situ bonding. This "bottom-up" strategy based on molecular design can ensure firm chemical bonding and efficient synergy among various functional modules [134]. The key to advancing new materials toward practical application is ensuring their stability in complex environments. Developing hydrogels that can tolerate extreme conditions remains an urgent and widespread challenge. Hydrogels tend to lose water, harden, and fail in dry settings, while in physiological fluids, they are prone to excessive swelling and structural damage. Stability can be enhanced through refined design strategies, such as introducing hydrophobic segments or microcrystalline domains to form physical crosslinks that help retain moisture and suppress evaporation, or employing dynamic covalent chemistry to create crosslinked networks capable of adaptive reorganization under osmotic pressure.

Traditional material discovery often relies on experience and trial-and-error [135]. Today, with the iteration of information technology and Artificial Intelligence (AI) driven material and structure design, materials science is shifting from a "trial-and-error experiment" paradigm to a new "data-driven" one [135]. AI, especially machine learning (ML) and deep learning (DL), has become a key driver due to its powerful data processing and prediction capabilities. It can significantly shorten the R&D cycle and promote material discovery and optimization [136]. AI shows great potential, especially in the fields of multi-functional devices and flexible electronics. For example, through generative adversarial networks (GANs) or reinforcement learning, composite materials with high conductivity, super elasticity, and self-healing capabilities can be designed, or lightweight and high-toughness bionic porous structures can be generated for wearable devices. However, the practical implementation of AI in materials design faces several challenges. These include the scarcity of large, high-quality, and well-annotated datasets required for training robust models; the "black-box" nature of many advanced ML/DL models, which limits interpretability and hinders the extraction of clear physical or chemical insights; and the often lengthy experimental validation cycles needed to bridge the gap between computational predictions and real-world material performance. In the future, with the in-depth integration of multi-scale simulation and AI, as well as the collaborative advancement of the Materials Genome

Initiative and automated experimental platforms (such as autonomous synthesis robots), AI is expected to become a core engine for breaking through the existing performance bottlenecks of materials and spurring disruptive technological applications [137–139].

Integrating multiple materials into a single structure enables a broader range of functions, allowing properties such as stiffness, flexibility, or optical dispersion to be fine-tuned within one component and multiple functions to be combined in a compact 3D architecture [102]. A major current limitation is the difficulty in simultaneously achieving micro- to nanoscale resolution, centimeter-scale printing area, and minute-level process efficiency in a single step. This challenge arises from the inherent trade-off between resolution and speed or area, coupled with a limited quantitative understanding of the coupling between ink rheology and cross-linking kinetics, which leaves process control largely dependent on empirical trial and error. The most advanced two-photon lithography systems, which operate on open-fluidic material-exchange principles, show promise for fabricating high-precision, free-form three-dimensional microstructures using multiple materials in a single printing run [140]. This approach incorporates automated in situ material switching without manual intervention, accelerating multi-material printing by an order of magnitude compared to conventional methods. Moreover, it is substrate independent and can print directly onto individual devices, existing components, or large wafers, regardless of their transparency, enabling a seamless workflow from design to final structure. To advance toward higher efficiency, template-free rapid prototyping technologies such as photothermally induced phase-separation three-dimensional printing are being explored [47]. This technique employs focused laser heating to trigger rapid sol-gel transitions in functional inks, facilitating the single-step shaping of complex geometries. By bypassing the masking or slicing-recoating steps required in conventional photocuring, it can reduce fabrication time from hours to tens of minutes, offering potential for scalable production.

A more influential cutting-edge direction is the activation of bioelectronic hydrogels. This approach embeds living cells or bioactive molecules as active components within 3D-printed hydrogel networks to construct integrated intelligent systems with "bionic sensing-active response" capabilities. For instance, Shi et al. incorporated living bacteria into hydrogels, leveraging their immunomodulatory functions along with the viscoelastic and bioelectrical properties of the hydrogel matrix, to achieve simultaneous inflammation monitoring, immune regulation, and biosafety management, thereby transcending the one-way signal-acquisition limits of conventional devices [141]. However, translating such bio-integrated systems into clinical practice faces substantial obstacles, primarily concerning long-term biosafety and complex regulatory pathways. Long-term biosafety involves potential immune responses, stability of the living components, and the biological fate of the composite material. Additionally, the combination of living biological elements with synthetic electronic parts creates intricate regulatory challenges that require rigorous preclinical validation and close collaboration with regulatory bodies. Future efforts should focus on advanced material strategies to enhance biocompatibility

and long-term safety, while establishing standardized characterization protocols and engaging with regulatory agencies early in the development process to define viable translational pathways for these innovative biohybrid systems.

## 6.2 Strategy for Synergistic Optimization of Sensing Performance via Hardware-Software Coordination

The core challenge faced by current flexible sensors is that their comprehensive performance still cannot meet the requirements of practical biomedical monitoring. On one hand, the sensitivity and detection limit of existing devices have obvious deficiencies. Their sensitivity is mostly limited to the range of 10–100, while the lower detection limits for strain and pressure are usually higher than 1% and 10 Pa, respectively. This performance shortcoming directly restricts the sensors' ability to capture key weak physiological signals such as cranial micro-vibrations and vascular pulse waves. On the other hand, during long-term dynamic monitoring, problems of signal drift and performance degradation caused by interface bonding failure and material fatigue itself have become increasingly prominent, which seriously affects the reliability and clinical value of monitoring data.

To break through the bottlenecks of sensitivity and detection limit, the focus of existing research is shifting from the development of a single material to a new model of collaborative design of structure and performance. By using DIW 3D printing technology, a multi-level bionic structure of micro-scale ceramic platelet alignment-bio-inspired macrostructure (unidirectional/Bouligand/cross-lamellar) is constructed. In this design, composite hydrogel filaments are assembled into biomimetic structures, and unidirectional arrangement and Bouligand structures are used to capture deformation signals. Microscopically, the oriented ceramic platelets in the filaments change their spacing and contact state with the matrix as the stress changes, thereby modulating the electrical signals. At the molecular level, hydrogen bonds and coordination bonds ensure the stability of this collaborative process [126]. In terms of material systems, the novel quaternary eutectic hydrogels exhibit the potential to break through the performance limits of traditional materials. Through elaborate molecular design, this type of material achieves a high sensitivity of up to 19.23 within a wide strain range of 0.1–500%, and this characteristic provides a new material basis for realizing both high sensitivity and a wide detection range simultaneously. Meanwhile, the excellent stability of quaternary eutectic hydrogels demonstrated in 2000 tensile cycles reveals the key role of dynamically reversible interactions in the anti-fatigue mechanism [145].

Regarding stability during long-term use, improving the interface bonding strength is the primary step to ensure signal reliability. Traditional physical adhesion methods are difficult to meet the application requirements in dynamic physiological environments, while chemical bonding strategies based on molecular grafting of transition layers and in-situ interface cross-linking are emerging as new solutions [146, 147]. The dopamine hydroxylated transition layer forms stable interface connections with the surfaces of different materials through its abundant functional groups, and the photo-initiated double

bond copolymerization technology can construct a covalent cross-linking network at the molecular level, essentially solving the problem of interface peeling under cyclic loads. These novel structural designs and mechanism studies provide a theoretical basis and technical pathway for increasing the cycle life of sensors to over hundreds of thousands of times, and lay a solid foundation for meeting the needs of long-term dynamic biomechanical monitoring.

In addition to improving stability at the physical level, the introduction of intelligent algorithms provides an additional guarantee for signal reliability. By developing self-calibration algorithms integrated with advanced models such as Convolutional Neural Network (CNN), the system can accurately extract target physiological features from mixed signals containing environmental interference and motion artifacts, enabling real-time correction of baseline drift and precise identification of health status [148]. This “hardware-software” synergy strategy effectively compensates for the limitations of relying solely on material improvements and provides new technical support for reliable monitoring in complex application scenarios.

## 6.3 Functional Integration in Medical Scenarios

3D-printed hydrogel flexible sensing technology shows great potential in laboratories, but its translation into clinical outcomes still faces severe challenges. In the field of healthcare, implantable and surface-mounted diagnosis and treatment devices need to simultaneously address long-term biological stability and reliability. Most hydrogel devices perform well in short-term experiments ranging from hours to days, yet the human body is a dynamic, complex, and aggressive chemical and physical environment. Long-term body fluid immersion, ion impact, enzymatic hydrolysis, and continuous mechanical deformation (e.g., joint bending, muscle contraction) can cause swelling, degradation, or mechanical fatigue of the hydrogel network, which in turn leads to sensing signal drift or even functional failure. Future research should focus on developing new hydrogel composites with stronger chemical cross-linking networks, anti-protein adsorption, and anti-degradation properties [149, 150]. Additionally, their long-term stability should be systematically evaluated through accelerated aging tests and in vitro models (e.g., simulated synovial fluid environment).

Second, achieving self-sufficiency in device energy and seamless data transmission is key to determining its clinical applicability. Solutions relying on external wires or frequent battery replacement are impractical in implantable or wearable medical scenarios. A future breakthrough lies in the integration of energy-harvesting units and sensing systems via 3D printing. Self-powered sensors are expected to be applied in integrated devices, playing a crucial role in enabling long-term, autonomous operation [151]. For instance, explore the use of the piezoelectric/triboelectric effect of hydrogels themselves to convert mechanical energy from physiological activities (e.g., heartbeat, pulse, walking) into electrical energy, or develop enzymatic biofuel cells based on biological fluids to continuously power microcircuits. Meanwhile,



## Author Contributions

Conceptualization, D.L.; Methodology, D.L. and L.J.; Validation, D.L., L.J. and Y.L.W.; Formal analysis, Z.W.S.; Investigation, D.L. and Y.L.W.; Resources, Z.L. and Q.Z.; Data curation, D.L.; Writing—original draft preparation, D.L.; Writing—review and editing, D.L., L.J. and Q.Z.; Visualization, Z.W.S. and Y.L.W.; Supervision, Z.L. and Q.Z.; Project administration, Q.Z.; Funding acquisition, Z.L. and Q.Z. All authors have read and agreed to the published version of the manuscript.

## Conflict of Interest

All the authors declare that they have no conflict of interest.

## Data Available

Data will be made available on request.

## References

- [1] Li, G., Li, C., Li, G., Yu, D., Song, Z., Wang, H., Liu, X., Liu, H., Liu, W.: Development of Conductive Hydrogels for Fabricating Flexible Strain Sensors. *Small* **18**(5), 2101518 (2021). <https://doi.org/10.1002/sml.202101518>
- [2] Zhu, T., Ni, Y., Biesold, G.M., Cheng, Y., Ge, M., Li, H., Huang, J., Lin, Z., Lai, Y.: Recent advances in conductive hydrogels: classifications, properties, and applications. *Chemical Society Reviews* **52**(2), 473–509 (2023). <https://doi.org/10.1039/D2CS00173J>
- [3] Zeng, X., Teng, L., Wang, X., Lu, T., Leng, W., Wu, X., Li, D., Zhong, Y., Sun, X., Zhu, S., et al.: Efficient multi-physical crosslinked nanocomposite hydrogel for a conformal strain and self-powered tactile sensor. *Nano Energy* **135**, 110669 (2025). <https://doi.org/10.1016/j.nanoen.2025.110669>
- [4] Wu, X., Yang, Z., Dong, Y., Teng, L., Li, D., Han, H., Zhu, S., Sun, X., Zeng, Z., Zeng, X., et al.: A Self-Powered, Skin Adhesive, and Flexible Human–Machine Interface Based on Triboelectric Nanogenerator. *Nanomaterials* **14**(16), 1365 (2024). <https://doi.org/10.3390/nano14161365>
- [5] Shi, Z., Meng, L., Shi, X., Li, H., Zhang, J., Sun, Q., Liu, X., Chen, J., Liu, S.: Morphological Engineering of Sensing Materials for Flexible Pressure Sensors and Artificial Intelligence Applications. *Nano-Micro Letters* **14**(1), 141 (2022). <https://doi.org/10.1007/s40820-022-00874-w>
- [6] Chen, S., Zhang, Y., Li, Y., Wang, P., Hu, D.: Recent development of flexible force sensors with multiple environmental adaptations. *Nano Energy* **124**, 109443 (2024). <https://doi.org/10.1016/j.nanoen.2024.109443>
- [7] Peng, S., Yu, Y., Wu, S., Wang, C.-H.: Conductive Polymer Nanocomposites for Stretchable Electronics: Material Selection, Design, and Applications. *ACS Applied Materials & Interfaces* **13**(37), 43831–43854 (2021). <https://doi.org/10.1021/acsami.1c15014>
- [8] Gong, S., Lu, Y., Yin, J., Levin, A., Cheng, W.: Materials-Driven Soft Wearable Bioelectronics for Connected Healthcare. *Chemical Reviews* **124**(2), 455–553 (2024). <https://doi.org/10.1021/acs.chemrev.3c00502>
- [9] Luo, Y., Abidian, M.R., Ahn, J.-H., Akinwande, D., Andrews, A.M., Antonietti, M., Bao, Z., Berggren, M., Berkey, C.A., Bettinger, C.J., et al.: Technology Roadmap for Flexible Sensors. *ACS Nano* **17**(6), 5211–5295 (2023). <https://doi.org/10.1021/acsnano.2c12606>
- [10] Raeisi, A., Farjadian, F.: Commercial hydrogel product for drug delivery based on route of administration. *Frontiers in Chemistry* **12**, 1336717 (2024). <https://doi.org/10.3389/fchem.2024.1336717>
- [11] Dey, K., Agnelli, S., Sartore, L.: Designing Viscoelastic Gelatin-PEG Macroporous Hybrid Hydrogel with Anisotropic Morphology and Mechanical Properties for Tissue Engineering Application. *Micro* **3**(2), 434–457 (2023). <https://doi.org/10.3390/micro3020029>
- [12] Liang, Y., He, J., Guo, B.: Functional Hydrogels as Wound Dressing to Enhance Wound Healing. *ACS Nano* **15**(8), 12687–12722 (2021). <https://doi.org/10.1021/acsnano.1c04206>
- [13] Amirthalingam, S., Rajendran, A.K., Moon, Y.G., Hwang, N.S.: Stimuli-responsive dynamic hydrogels: design, properties and tissue engineering applications. *Materials Horizons* **10**(9), 3325–3350 (2023). <https://doi.org/10.1039/D3MH00399J>
- [14] Cheng, L., Suresh K, S., He, H., Rajput, R.S., Feng, Q., Ramesh, S., Wang, Y., Krishnan, S., Ostrovidov, S., Camci-Unal, G., et al.: 3D Printing of Micro- and Nanoscale Bone Substitutes: A Review on Technical and Translational Perspectives. *International Journal of Nanomedicine* **16**, 4289–4319 (2021). <https://doi.org/10.2147/ijn.s311001>
- [15] Murab, S., Gupta, A., Włodarczyk-Biegun, M.K., Kumar, A., van Rijn, P., Whitlock, P., Han, S.S., Agrawal, G.: Alginate based hydrogel inks for 3D bioprinting of engineered orthopedic tissues. *Carbohydrate Polymers* **296**, 119964 (2022). <https://doi.org/10.1016/j.carbpol.2022.119964>
- [16] Zhu, Z., Ng, D.W.H., Park, H.S., McAlpine, M.C.: 3D-printed multifunctional materials enabled by artificial-intelligence-assisted fabrication technologies. *Nature Reviews Materials* **6**, 27–47 (2021). <https://doi.org/10.1038/s41578-020-00235-2>

- [17] Seoane-Viaño, I., Januskaite, P., Alvarez-Lorenzo, C., Basit, A.W., Goyanes, A.: Semi-solid extrusion 3D printing in drug delivery and biomedicine: Personalised solutions for healthcare challenges. *Journal of Controlled Release* **332**, 367–389 (2021). <https://doi.org/10.1016/j.jconrel.2021.02.027>
- [18] Sun, J., Liu, Q., Yang, J.: Additive manufacturing of highly entangled polymer networks. *Science* **385**(6708), 566–572 (2024). <https://doi.org/10.1126/science.adn6925>
- [19] Li, J., Cao, J., Bian, R., Wan, R., Zhu, X., Lu, B., Gu, G.: Multimaterial cryogenic printing of three-dimensional soft hydrogel machines. *Nature Communications* **16**(1), 185 (2025). <https://doi.org/10.1038/s41467-024-55323-6>
- [20] Ji, Y., Su, E., Yee, D.W.: Volumetric Additive Manufacturing of Composites via Hydrogel Infusion. *ACS Materials Letters* **7**(8), 2850–2857 (2025). <https://doi.org/10.1021/acsmaterialslett.5c00407>
- [21] Daly, A.C., Davidson, M.D., Burdick, J.A.: 3D bioprinting of high cell-density heterogeneous tissue models through spheroid fusion within self-healing hydrogels. *Nature Communications* **12**(1), 753 (2021). <https://doi.org/10.1038/s41467-021-21029-2>
- [22] Lin, X., Teng, Y., Xue, H., Bing, Y., Li, F., Wang, J., Li, J., Zhao, H., Zhang, T.: Janus Conductive Mechanism: An Innovative Strategy Enabling Ultra-Wide Linearity Range Pressure Sensing for Multi-Scenario Applications. *Advanced Functional Materials* **34**(32), 2316314 (2024). <https://doi.org/10.1002/adfm.202316314>
- [23] Li, G., Chu, Z., Gong, X., Xiao, M., Dong, Q., Zhao, Z., Hu, T., Zhang, Y., Wang, J., Tan, Y., et al.: A Wide-Range Linear and Stable Piezoresistive Sensor Based on Methylcellulose-Reinforced, Lamellar, and Wrinkled Graphene Aerogels. *Advanced Materials Technologies* **7**(5), 2101021 (2021). <https://doi.org/10.1002/admt.202101021>
- [24] Zhu, G., Dai, H., Yao, Y., Tang, W., Shi, J., Yang, J., Zhu, L.: 3D Printed Skin-Inspired Flexible Pressure Sensor with Gradient Porous Structure for Tunable High Sensitivity and Wide Linearity Range. *Advanced Materials Technologies* **7**(7), 2101239 (2021). <https://doi.org/10.1002/admt.202101239>
- [25] Shu, Q., Pang, Y., Li, Q., Gu, Y., Liu, Z., Liu, B., Li, J., Li, Y.: Flexible resistive tactile pressure sensors. *Journal of Materials Chemistry A* **12**(16), 9296–9321 (2024). <https://doi.org/10.1039/D3TA06976A>
- [26] Wackers, G., Putzeys, T., Peeters, M., Van de Cauter, L., Cornelis, P., Wübbenhorst, M., Tack, J., Troost, F., Verhaert, N., Doll, T., et al.: Towards a catheter-based impedimetric sensor for the assessment of intestinal histamine levels in IBS patients. *Biosensors and Bioelectronics* **158**, 112152 (2020). <https://doi.org/10.1016/j.bios.2020.112152>
- [27] Zhao, S., Liu, D., Yan, F.: Wearable Resistive-Type Stretchable Strain Sensors: Materials and Applications. *Advanced Materials* **37**(5), 2413929 (2024). <https://doi.org/10.1002/adma.202413929>
- [28] Hu, R., Liu, P., Zhu, W., Guo, X., Liu, Z., Jin, Z., Yang, R., Han, J., Tian, H., Ma, Y., et al.: Design, Fabrication, and Wearable Medical Application of a High-Resolution Flexible Capacitive Temperature Sensor Based on the Thermotropic Phase Transition Composites of PEO/PVDF-HFP/H3PO4. *Advanced Functional Materials* **35**(11), 2417205 (2024). <https://doi.org/10.1002/adfm.202417205>
- [29] Qin, J., Yin, L.J., Hao, Y.N., Zhong, S.L., Zhang, D.L., Bi, K., Zhang, Y.X., Zhao, Y., Dang, Z.M.: Flexible and Stretchable Capacitive Sensors with Different Microstructures. *Advanced Materials* **33**(34), 2008267 (2021). <https://doi.org/10.1002/adma.202008267>
- [30] Tay, R.Y., Li, H., Lin, J., Wang, H., Lim, J.S.K., Chen, S., Leong, W.L., Tsang, S.H., Teo, E.H.T.: Lightweight, Superelastic Boron Nitride/Polydimethylsiloxane Foam as Air Dielectric Substitute for Multifunctional Capacitive Sensor Applications. *Advanced Functional Materials* **30**(10), 1909604 (2020). <https://doi.org/10.1002/adfm.201909604>
- [31] Ma, Z., Zhang, Y., Zhang, K., Deng, H., Fu, Q.: Recent progress in flexible capacitive sensors: Structures and properties. *Nano Materials Science* **5**(3), 265–277 (2023). <https://doi.org/10.1016/j.nanoms.2021.11.002>
- [32] Basarir, F., Haj, Y.A., Zou, F., De, S., Nguyen, A., Frey, A., Haider, I., Sariola, V., Vapaavuori, J.: Edible and Biodegradable Wearable Capacitive Pressure Sensors: A Paradigm Shift toward Sustainable Electronics with Bio-Based Materials. *Advanced Functional Materials* **34**(39), 2403268 (2024). <https://doi.org/10.1002/adfm.202403268>
- [33] Qin, R., Hu, M., Li, X., Liang, T., Tan, H., Liu, J., Shan, G.: A new strategy for the fabrication of a flexible and highly sensitive capacitive pressure sensor. *Microsystems & Nanoengineering* **7**(1), 100 (2021). <https://doi.org/10.1038/s41378-021-00327-1>
- [34] Basarir, F., Madani, Z., Vapaavuori, J.: Recent Advances in Silver Nanowire Based Flexible Capacitive Pressure Sensors: From Structure, Fabrication to Emerging Applications. *Advanced Materials Interfaces* **9**(31), 2200866 (2022). <https://doi.org/10.1002/admi.202200866>
- [35] Mariello, M., Fachechi, L., Guido, F., De Vittorio, M.: Conformal, Ultra-thin Skin-Contact-Actuated Hybrid Piezo/Triboelectric Wearable Sensor Based on AlN and

- Parylene-Encapsulated Elastomeric Blend. *Advanced Functional Materials* **31**(27), 2101047 (2021). <https://doi.org/10.1002/adfm.202101047>
- [36] Li, Y., Luo, Y., Deng, H., Shi, S., Tian, S., Wu, H., Tang, J., Zhang, C., Zhang, X., Zha, J.W., et al.: Advanced Dielectric Materials for Triboelectric Nanogenerators: Principles, Methods, and Applications. *Advanced Materials* **36**(52), 2314380 (2024). <https://doi.org/10.1002/adma.202314380>
- [37] Dassanayaka, D.G., Alves, T.M., Wanasekara, N.D., Dharmasena, I.G., Ventura, J.: Recent Progresses in Wearable Triboelectric Nanogenerators. *Advanced Functional Materials* **32**(44), 2205438 (2022). <https://doi.org/10.1002/adfm.202205438>
- [38] Deng, W., Yang, T., Jin, L., Yan, C., Huang, H., Chu, X., Wang, Z., Xiong, D., Tian, G., Gao, Y., et al.: Cowpea-structured PVDF/ZnO nanofibers based flexible self-powered piezoelectric bending motion sensor towards remote control of gestures. *Nano Energy* **55**, 516–525 (2019). <https://doi.org/10.1016/j.nanoen.2018.10.049>
- [39] Yang, L., Liu, Q., Li, M., Liu, Y., Li, X., Liu, Q., Zhu, T., Lu, Y., Liu, X., Wang, D.: A high-performance, flexible, and dual-modal humidity-piezoelectric sensor without mutual interference. *Sensors and Actuators B: Chemical* **423**, 136778 (2025). <https://doi.org/10.1016/j.snb.2024.136778>
- [40] Chen, Y., Qin, C., Sun, Q., Wang, M.: Arrayed multi-layer piezoelectric sensor based on electrospun P(VDF-TrFE)/ZnO with enhanced piezoelectricity. *Sensors and Actuators A: Physical* **379**, 115970 (2024). <https://doi.org/10.1016/j.sna.2024.115970>
- [41] Cao, C., Zhou, P., Qin, W., Wang, J., Liu, M., Wang, P., Zhang, T., Qi, Y.: Enhanced sensing performance of piezoelectric pressure sensors via integrated nanofillers incorporated with P(VDF-TrFE) composites. *Applied Surface Science* **685**, 162028 (2025). <https://doi.org/10.1016/j.apsusc.2024.162028>
- [42] Zhen, L., Cui, M., Bai, X., Jiang, J., Ma, X., Wang, M., Liu, J., Yang, B.: Thin, flexible hybrid-structured piezoelectric sensor array with enhanced resolution and sensitivity. *Nano Energy* **131**, 110188 (2024). <https://doi.org/10.1016/j.nanoen.2024.110188>
- [43] Yin, B., Gosecka, M., Bodaghi, M., Crespy, D., Youssef, G., Dodda, J.M., Wong, S.H.D., Imran, A.B., Gosecki, M., Jobdeedamrong, A., et al.: Engineering multifunctional dynamic hydrogel for biomedical and tissue regenerative applications. *Chemical Engineering Journal* **487**, 150403 (2024). <https://doi.org/10.1016/j.cej.2024.150403>
- [44] Zhang, Y., Tan, Y., Lao, J., Gao, H., Yu, J.: Hydrogels for Flexible Electronics. *ACS Nano* **17**(11), 9681–9693 (2023). <https://doi.org/10.1021/acsnano.3c02897>
- [45] Li, H., Cao, J., Wan, R., Feig, V.R., Tringides, C.M., Xu, J., Yuk, H., Lu, B.: PEDOTs-Based Conductive Hydrogels: Design, Fabrications, and Applications. *Advanced Materials* **37**(7), 2415151 (2024). <https://doi.org/10.1002/adma.202415151>
- [46] Fatih, P., Karen, L.: 3D Printing of Polymer Hydrogels—From Basic Techniques to Programmable Actuation. *Advanced Functional Materials* **32**(39), 2205345 (2022). <https://doi.org/10.1002/adfm.202205345>
- [47] He, X., Zhang, B., Liu, Q., Chen, H., Cheng, J., Jian, B., Yin, H., Li, H., Duan, K., Zhang, J., et al.: Highly conductive and stretchable nanostructured ionogels for 3D printing capacitive sensors with superior performance. *Nature Communications* **15**(1), 6431 (2024). <https://doi.org/10.1038/s41467-024-50797-w>
- [48] Dhand, A.P., Davidson, M.D., Burdick, J.A.: Lithography-based 3D printing of hydrogels. *Nature Reviews Bioengineering* **3**(2), 108–125 (2024). <https://doi.org/10.1038/s44222-024-00251-9>
- [49] Zhu, Z., Park, H.S., McAlpine, M.C.: 3D printed deformable sensors. *Science Advances* **6**(25), eaba5575 (2020). <https://doi.org/10.1126/sciadv.aba5575>
- [50] Sun, Y., Kumar, V., Adesida, I., Rogers, J.A.: Buckled and Wavy Ribbons of GaAs for High-Performance Electronics on Elastomeric Substrates. *Advanced Materials* **18**(21), 2857–2862 (2006). <https://doi.org/10.1002/adma.200600646>
- [51] Mannsfeld, S.C.B., Tee, B.C.K., Stoltenberg, R.M., Chen, C.V.H.H., Barman, S., Muir, B.V.O., Sokolov, A.N., Reese, C., Bao, Z.: Highly sensitive flexible pressure sensors with microstructured rubber dielectric layers. *Nature Materials* **9**(10), 859–864 (2010). <https://doi.org/10.1038/nmat2834>
- [52] Lipomi, D.J., Vosgueritchian, M., Tee, B.C.K., Hellstrom, S.L., Lee, J.A., Fox, C.H., Bao, Z.: Skin-like pressure and strain sensors based on transparent elastic films of carbon nanotubes. *Nature Nanotechnology* **6**(12), 788–792 (2011). <https://doi.org/10.1038/nnano.2011.184>
- [53] Fan, F.-R., Lin, L., Zhu, G., Wu, W., Zhang, R., Wang, Z.L.: Transparent Triboelectric Nanogenerators and Self-Powered Pressure Sensors Based on Micropatterned Plastic Films. *Nano Letters* **12**(6), 3109–3114 (2012). <https://doi.org/10.1021/nl300988z>
- [54] Chun, J., Lee, K.Y., Kang, C.Y., Kim, M.W., Kim, S.W., Baik, J.M.: Embossed Hollow Hemisphere-Based Piezoelectric Nanogenerator and Highly Responsive Pressure Sensor. *Advanced Functional Materials* **24**(14), 2038–2043 (2013). <https://doi.org/10.1002/adfm.201302962>

- [55] Shao, Q., Niu, Z., Hirtz, M., Jiang, L., Liu, Y., Wang, Z., Chen, X.: High-Performance and Tailorable Pressure Sensor Based on Ultrathin Conductive Polymer Film. *Small* **10**(8), 1466–1472 (2014). <https://doi.org/10.1002/smll.201303601>
- [56] Lee, J., Kwon, H., Seo, J., Shin, S., Koo, J.H., Pang, C., Son, S., Kim, J.H., Jang, Y.H., Kim, D.E., et al.: Conductive Fiber-Based Ultrasensitive Textile Pressure Sensor for Wearable Electronics. *Advanced Materials* **27**(15), 2433–2439 (2015). <https://doi.org/10.1002/adma.201500009>
- [57] Wang, Z., Wang, S., Zeng, J., Ren, X., Chee, A.J.Y., Yiu, B.Y.S., Chung, W.C., Yang, Y., Yu, A.C.H., Roberts, R.C., et al.: High Sensitivity, Wearable, Piezoresistive Pressure Sensors Based on Irregular Microhump Structures and Its Applications in Body Motion Sensing. *Small* **12**(28), 3827–3836 (2016). <https://doi.org/10.1002/smll.201601419>
- [58] Luo, N., Huang, Y., Liu, J., Chen, S.C., Wong, C.P., Zhao, N.: Hollow-Structured Graphene–Silicone-Composite-Based Piezoresistive Sensors: Decoupled Property Tuning and Bending Reliability. *Advanced Materials* **29**(40), 1702675 (2017). <https://doi.org/10.1002/adma.201702675>
- [59] Chun, S., Son, W., Choi, C.: Flexible pressure sensors using highly-oriented and free-standing carbon nanotube sheets. *Carbon* **139**, 586–592 (2018). <https://doi.org/10.1016/j.carbon.2018.07.005>
- [60] Chang, Q., Darabi, M.A., Liu, Y., He, Y., Zhong, W., Mequanin, K., Li, B., Lu, F., Xing, M.M.Q.: Hydrogels from natural egg white with extraordinary stretchability, direct-writing 3D printability and self-healing for fabrication of electronic sensors and actuators. *Journal of Materials Chemistry A* **7**(42), 24626–24640 (2019). <https://doi.org/10.1039/C9TA06233E>
- [61] Wu, Y., Zeng, Y., Chen, Y., Li, C., Qiu, R., Liu, W.: Photocurable 3D Printing of High Toughness and Self-Healing Hydrogels for Customized Wearable Flexible Sensors. *Advanced Functional Materials* **31**(52), 2107202 (2021). <https://doi.org/10.1002/adfm.202107202>
- [62] Haodong, L., Chunyu, D., Liling, L., Hongjian, Z., Haiqing, Z., Weichang, Z., Tianning, R., Zhicheng, S., Yuquan, L., Zhentao, N., et al.: Approaching intrinsic dynamics of MXenes hybrid hydrogel for 3D printed multimodal intelligent devices with ultrahigh superelasticity and temperature sensitivity. *Nature Communications* **13**(1), 3420 (2022). <https://doi.org/10.1038/s41467-022-31051-7>
- [63] Jingxia, Z., Guoqi, C., Hongjuan, Y., Canjie, Z., Shengnan, L., Wenquan, W., Jiangtao, R., Yang, C., Xun, X., Xinwei, W., et al.: 3D printed microstructured ultrasensitive pressure sensors based on microgel-reinforced double network hydrogels for biomechanical applications. *Materials Horizons* **10**(10), 4232–4242 (2023). <https://doi.org/10.1039/D3MH00718A>
- [64] Tang, H., Yang, Y., Liu, Z., Li, W., Zhang, Y., Huang, Y., Kang, T., Yu, Y., Li, N., Tian, Y., et al.: Injectable ultrasonic sensor for wireless monitoring of intracranial signals. *Nature* **630**(8015), 84–90 (2024). <https://doi.org/10.1038/s41586-024-07334-y>
- [65] Zhou, X., Yu, X., You, T., Zhao, B., Dong, L., Huang, C., Zhou, X., Xing, M., Qian, W., Luo, G.: 3D Printing-Based Hydrogel Dressings for Wound Healing. *Advanced Science* **11**(47), 2404580 (2024). <https://doi.org/10.1002/advs.202404580>
- [66] Vijayavenkataraman, S., Yan, W.-C., Lu, W.F., Wang, C.-H., Fuh, J.Y.H.: 3D bioprinting of tissues and organs for regenerative medicine. *Advanced Drug Delivery Reviews* **132**, 296–332 (2018). <https://doi.org/10.1016/j.addr.2018.07.004>
- [67] Ho, M., Ramirez, A.B., Akbarnia, N., Croiset, E., Prince, E., Fuller, G.G., Kamkar, M.: Direct Ink Writing of Conductive Hydrogels. *Advanced Functional Materials* **35**(22), 2404580 (2025). <https://doi.org/10.1002/adfm.202415507>
- [68] Baniasadi, H., Abidnejad, R., Fazeli, M., Lipponen, J., Niskanen, J., Kontturi, E., Seppälä, J., Rojas, O.J.: Innovations in hydrogel-based manufacturing: A comprehensive review of direct ink writing technique for biomedical applications. *Advances in Colloid and Interface Science* **324**, 103095 (2024). <https://doi.org/10.1016/j.cis.2024.103095>
- [69] Shahzad, A., Lazoglu, I.: Direct ink writing (DIW) of structural and functional ceramics: Recent achievements and future challenges. *Composites Part B: Engineering* **225**, 109249 (2021). <https://doi.org/10.1016/j.compositesb.2021.109249>
- [70] Wu, Y., Zhang, Y., Yan, M., Hu, G., Li, Z., He, W., Wang, X., Abulimit, A., Li, R.: Research progress on the application of inkjet printing technology combined with hydrogels. *Applied Materials Today* **36**, 102036 (2024). <https://doi.org/10.1016/j.apmt.2023.102036>
- [71] Shah, M.A., Lee, D.-G., Lee, B.-Y., Hur, S.: Classifications and Applications of Inkjet Printing Technology: A Review. *IEEE Access* **9**, 140079–140102 (2021). <https://doi.org/10.1109/ACCESS.2021.3119219>
- [72] Cheng, C., Williamson, E.J., Chiu, G.T.C., Han, B.: Engineering biomaterials by inkjet printing of hydrogels with functional particulates. *Med-X* **2**(1), 9 (2024). <https://doi.org/10.1007/s44258-024-00024-4>
- [73] Teo, M.Y., Kee, S., RaviChandran, N., Stuart, L., Aw, K.C., Stringer, J.: Enabling Free-Standing 3D Hydrogel Microstructures with Microreactive Inkjet Printing.

- ACS Applied Materials & Interfaces **12**(1), 1832–1839 (2019). <https://doi.org/10.1021/acsami.9b17192>
- [74] Quan, H., Zhang, T., Xu, H., Luo, S., Nie, J., Zhu, X.: Photo-curing 3D printing technique and its challenges. *Bioactive Materials* **5**(1), 110–115 (2020). <https://doi.org/10.1016/j.bioactmat.2019.12.003>
- [75] Dhand, A.P., Davidson, M.D., Zlotnick, H.M., Kolibaba, T.J., Killgore, J.P., Burdick, J.A.: Additive manufacturing of highly entangled polymer networks. *Science* **385**(6708), 566–572 (2024). <https://doi.org/10.1126/science.adn6925>
- [76] Ouyang, L.: Pushing the rheological and mechanical boundaries of extrusion-based 3D bioprinting. *Trends in Biotechnology* **40**(7), 891–902 (2022). <https://doi.org/10.1016/j.tibtech.2022.01.001>
- [77] Bedell, M.L., Navara, A.M., Du, Y., Zhang, S., Mikos, A.G.: Polymeric Systems for Bioprinting. *Chemical Reviews* **120**(19), 10744–10792 (2020). <https://doi.org/10.1021/acs.chemrev.9b00834>
- [78] Piras, C.C., Smith, D.K.: Multicomponent polysaccharide alginate-based bioinks. *Journal of Materials Chemistry B* **8**(36), 8171–8188 (2020). <https://doi.org/10.1039/D0TB01005G>
- [79] Hasany, M., Talebian, S., Sadat, S., Ranjbar, N., Mehrali, M., Wallace, G.G., Mehrali, M.: Synthesis, properties, and biomedical applications of alginate methacrylate (ALMA)-based hydrogels: Current advances and challenges. *Applied Materials Today* **24**, 101150 (2021). <https://doi.org/10.1016/j.apmt.2021.101150>
- [80] Lee, S., Choi, G., Yang, Y.J., Joo, K.I., Cha, H.J.: Visible light-crosslinkable tyramine-conjugated alginate-based microgel bioink for multiple cell-laden 3D artificial organ. *Carbohydrate Polymers* **313**, 120895 (2023). <https://doi.org/10.1016/j.carbpol.2023.120895>
- [81] Agostinacchio, F., Fitzpatrick, V., Dirè, S., Kaplan, D.L., Motta, A.: Silk fibroin-based inks for in situ 3D printing using a double crosslinking process. *Bioactive Materials* **35**, 122–134 (2024). <https://doi.org/10.1016/j.bioactmat.2024.01.015>
- [82] Yan, X., Huang, H., Bakry, A.M., Wu, W., Liu, X., Liu, F.: Advances in enhancing the mechanical properties of biopolymer hydrogels via multi-strategic approaches. *International Journal of Biological Macromolecules* **272**, 132583 (2024). <https://doi.org/10.1016/j.ijbiomac.2024.132583>
- [83] Liu, X., Hao, S., Wang, Y., Zheng, L., Hu, Z., Wen, J., Xu, F., Yang, J.: Mechanically adaptable microdomed hydrogels for flexible pressure sensors with broad detection range and stable signal output. *Chemical Engineering Journal* **505**, 159113 (2025). <https://doi.org/10.1016/j.ccej.2024.159113>
- [84] Yang, S., Pan, J., Fu, H., Zheng, J., Chen, F., Zhang, M., Gong, Z., Liang, K., Wang, C., Lai, J., et al.: Preparation of carbon-based conductive hydrogels and their potential for promoting nerve regeneration. *Advanced Composites and Hybrid Materials* **8**(2), 185 (2025). <https://doi.org/10.1007/s42114-025-01261-w>
- [85] Deng, W., Zhang, Y., Wu, M., Liu, C., Rahmaninia, M., Tang, Y., Li, B.: A tough, stretchable, adhesive and electroconductive polyacrylamide hydrogel sensor incorporated with sulfonated nanocellulose and carbon nanotubes. *International Journal of Biological Macromolecules* **279**, 135165 (2024). <https://doi.org/10.1016/j.ijbiomac.2024.135165>
- [86] Liu, P., Yao, D., Lu, C., Gao, X., Dong, P.: Highly sensitive strain sensors based on PVA hydrogels with a conductive surface layer of graphene. *Journal of Materials Science: Materials in Electronics* **35**(2), 97 (2024). <https://doi.org/10.1007/s10854-024-11927-8>
- [87] Zhou, T., Yuk, H., Hu, F., Wu, J., Tian, F., Roh, H., Shen, Z., Gu, G., Xu, J., Lu, B., et al.: 3D printable high-performance conducting polymer hydrogel for all-hydrogel bioelectronic interfaces. *Nature Materials* **22**(7), 895–902 (2023). <https://doi.org/10.1038/s41563-023-01569-2>
- [88] GhavamiNejad, A., Ashammakhi, N., Wu, X.Y., Khademhosseini, A.: Crosslinking Strategies for 3D Bioprinting of Polymeric Hydrogels. *Small* **16**(35), 2002931 (2020). <https://doi.org/10.1002/smll.202002931>
- [89] Zeng, L., Wang, J., Duan, L., Gao, G.: Highly transparent ionogel for wearable force sensor and 3D printing. *European Polymer Journal* **223**, 113641 (2025). <https://doi.org/10.1016/j.eurpolymj.2024.113641>
- [90] Zhu, L., Rong, Y., Wang, Y., Bao, Q., An, J., Huang, D., Huang, X.: DLP printing of tough organogels for customized wearable sensors. *European Polymer Journal* **187**, 111886 (2023). <https://doi.org/10.1016/j.eurpolymj.2023.111886>
- [91] Liu, S., Zhang, H., Ahlfeld, T., Kilian, D., Liu, Y., Gelinsky, M., Hu, Q.: Evaluation of different crosslinking methods in altering the properties of extrusion-printed chitosan-based multi-material hydrogel composites. *Bio-Design and Manufacturing* **6**(2), 150–173 (2023). <https://doi.org/10.1007/s42242-022-00194-3>
- [92] Ouyang, L., Armstrong, J.P.K., Lin, Y., Wojciechowski, J.P., Lee-Reeves, C., Hachim, D., Zhou, K., Burdick, J.A., Stevens, M.M.: Expanding and optimizing 3D bioprinting capabilities using complementary network bioinks. *Science Advances* **6**(38), eabc5529 (2020). <https://doi.org/10.1126/sciadv.abc5529>

- [93] Zhang, X., Li, D., Liu, G.: 3D Printed Ultrasoft and Adhesive PEDOT:PSS-Based Hydrogel for Bioelectronics. *ACS Applied Polymer Materials* **7**(3), 1531–1539 (2025). <https://pubs.acs.org/doi/10.1021/acsapm.4c03275>
- [94] Choi, S., Lee, K.Y., Kim, S.L., MacQueen, L.A., Chang, H., Zimmerman, J.F., Jin, Q., Peters, M.M., Ardoña, H.A.M., Liu, X., et al.: Fibre-infused gel scaffolds guide cardiomyocyte alignment in 3D-printed ventricles. *Nature Materials* **22**(8), 1039–1046 (2023). <https://doi.org/10.1038/s41563-023-01611-3>
- [95] Guo, B., Lin, C., Ye, H., Xue, Y., Mo, J., Chen, J., Cui, Y., Fu, C., Bai, J., Ge, Q., et al.: 3D printed organohydrogel-based strain sensors with enhanced sensitivity and stability via structural design. *International Journal of Extreme Manufacturing* **7**(5), 055507 (2025). <https://doi.org/10.1088/2631-7990/add971>
- [96] Wang, Y., Okuro, K.: Mechano-Chemiluminescent Hydrogel for Sustained Stress Visualization Under Mechanical Equilibrium. *Macromolecular Rapid Communications* **46**(19), 2500256 (2025). <https://doi.org/10.1002/marc.202500256>
- [97] Barrulas, R.V., Corvo, M.C.: Rheology in Product Development: An Insight into 3D Printing of Hydrogels and Aerogels. *Gels* **9**(12), 986 (2023). <https://doi.org/10.3390/gels9120986>
- [98] Cook-Chennault, K., Anaokar, S., Medina Vázquez, A.M., Chennault, M.: Influence of High Strain Dynamic Loading on HEMA–DMAEMA Hydrogel Storage Modulus and Time Dependence. *Polymers* **16**(13), 1797 (2024). <https://doi.org/10.3390/polym16131797>
- [99] Zhang, L., Bai, X., Liang, Y., Zhang, G., Zou, J., Lai, W., Fei, P.: Preparation of chitosan derivatives/oxidized carboxymethyl cellulose hydrogels by freeze-thaw method: Synthesis, characterization, and utilization in dye absorption. *International Journal of Biological Macromolecules* **282**, 136924 (2024). <https://doi.org/10.1016/j.ijbiomac.2024.136924>
- [100] Liu, P., Zhang, Y., Guan, Y., Zhang, Y.: Peptide-Crosslinked, Highly Entangled Hydrogels with Excellent Mechanical Properties but Ultra-Low Solid Content. *Advanced Materials* **35**(13), 2210021 (2023). <https://doi.org/10.1002/adma.202210021>
- [101] Podder, A.K., Mohamed, M.A., Seidman, R.A., Tseropoulos, G., Polanco, J.J., Lei, P., Sim, F.J., Andreadis, S.T.: Injectable shear-thinning hydrogels promote oligodendrocyte progenitor cell survival and remyelination in the central nervous system. *Science Advances* **10**(28), eadk9918 (2024). <https://doi.org/10.1126/sciadv.adk9918>
- [102] Brown, N.C., Ames, D.C., Mueller, J.: Multimaterial extrusion 3D printing printheads. *Nature Reviews Materials* **10**, 807–825 (2025). <https://doi.org/10.1038/s41578-025-00809-y>
- [103] Guvendiren, M., Lu, H.D., Burdick, J.A.: Shear-thinning hydrogels for biomedical applications. *Soft Matter* **8**(2), 260–272 (2012). <https://doi.org/10.1039/C1SM06513K>
- [104] Yuan, Z., Huang, X., Zhang, X., Gao, S., Chen, H., Li, Z., El-Mesery, H.S., Shi, J., Zou, X.: Unveiling rheological behavior of hydrogels toward Magic 3D printing patterns. *Food Hydrocolloids* **168**, 111505 (2025). <https://doi.org/10.1016/j.foodhyd.2025.111505>
- [105] Kang, S.W., Mueller, J.: Multiscale 3D printing via active nozzle size and shape control. *Science Advances* **10**(23), eadn7772 (2024). <https://doi.org/10.1126/sciadv.adn7772>
- [106] Bono, F., Strassle Zuniga, S.H., Amstad, E.: 3D Printable k-Carrageenan-Based Granular Hydrogels. *Advanced Functional Materials* **35**(3), 2413368 (2024). <https://doi.org/10.1002/adfm.202413368>
- [107] Ge, Q., Chen, Z., Cheng, J., Zhang, B., Zhang, Y.-F., Li, H., He, X., Yuan, C., Liu, J., Magdassi, S., et al.: 3D printing of highly stretchable hydrogel with diverse UV curable polymers. *Science Advances* **7**(2), eaba4261 (2021). <https://doi.org/10.1126/sciadv.aba4261>
- [108] Highley, C.B., Rodell, C.B., Burdick, J.A.: Direct 3D Printing of Shear-Thinning Hydrogels into Self-Healing Hydrogels. *Advanced Materials* **27**(34), 5075–5079 (2015). <https://doi.org/10.1002/adma.201501234>
- [109] Khan, K., Hussain, M.I., Tareen, A.K., Asghar, A., Hamza, M., Chen, Z.: Advances in vat photopolymerization 3D printing: Multifunctional materials, process innovations, and emerging applications. *Materials Science and Engineering: R: Reports* **167**, 101120 (2026). <https://doi.org/10.1016/j.msere.2025.101120>
- [110] Wu, R., Zhu, T., Ni, Y., Wu, C., Wang, W., Zhao, K., Huang, J., Lai, Y.: UV-Cured Dense Double Network Hydrogel via Multiple Dynamic Crosslinking for Stable Amphibious Motion Sensing. *Advanced Functional Materials* **36**(3), e15120 (2025). <https://doi.org/10.1002/adfm.202515120>
- [111] Li, Q., Zhao, Y.L., Shen, H.X., Hou, Y.C., Lu, J.L., Zhu, L., Chen, S.: 3D Printing–In Situ Curing of Soft Organogels Using Frontal Polymerizable Inks. *Advanced Materials* **37**(35), 2419039 (2025). <https://doi.org/10.1002/adma.202419039>
- [112] Ye, T., Chai, M., Wang, Z., Shao, T., Liu, J., Shi, X.: 3D-Printed Hydrogels with Engineered Nanocrystalline Domains as Functional Vascular Constructs. *ACS Nano* **18**(37), 25765–25777 (2024). <https://doi.org/10.1021/acsnano.4c08359>

- [113] Wang, Y., Xu, X., Liu, D., Wu, J., Yang, X., Zhu, B., Sun, C., Jiang, P., Wang, X.: Dimethyl sulfoxide mediated high-fidelity 3D printing of hydrogels. *Additive Manufacturing* **91**, 104346 (2024). <https://doi.org/10.1016/j.addma.2024.104346>
- [114] Zhuo, S., Qian, Z., Sainan, M., Jingjun, W.: DLP 3D printed hydrogels with hierarchical structures post-programmed by lyophilization and ionic locking. *Materials Horizons* **10**(1), 179–186 (2023). <https://doi.org/10.1039/D2MH00962E>
- [115] Cui, C., Zhuang, Z.Y., Gao, H.L., Pang, J., Pan, X.F., Yu, S.H.: 3D Printing of Ultrahigh Filler Content Composites Enabled by Granular Hydrogels. *Advanced Materials* **37**(30), 2500782 (2025). <https://doi.org/10.1002/adma.202500782>
- [116] Wang, F., Xue, Y., Chen, X., Zhang, P., Shan, L., Duan, Q., Xing, J., Lan, Y., Lu, B., Liu, J.: 3D Printed Implantable Hydrogel Bioelectronics for Electrophysiological Monitoring and Electrical Modulation. *Advanced Functional Materials* **34**(21), 2314471 (2023). <https://doi.org/10.1002/adfm.202470116>
- [117] Wang, Z., Chen, L., Chen, Y., Liu, P., Duan, H., Cheng, P.: 3D Printed Ultrastretchable, Hyper-Antifreezing Conductive Hydrogel for Sensitive Motion and Electrophysiological Signal Monitoring. *Research* **2020**, 1426078 (2020). <https://doi.org/10.34133/2020/1426078>
- [118] Zheng, S., Ruan, L., Meng, F., Wu, Z., Qi, Y., Gao, Y., Yuan, W.: Skin-Inspired, Multifunctional, and 3D-Printable Flexible Sensor Based on Triple-Responsive Hydrogel for Signal Conversion in Skin Interface Electronics Health Management. *Small* **21**(6), 2408745 (2024). <https://doi.org/10.1002/sml.202408745>
- [119] Tang, J., Gou, K., Wang, C., Wei, M., Tan, Q., Weng, G.: Self-Powered and 3D Printable Soft Sensor for Human Health Monitoring, Object Recognition, and Contactless Hand Gesture Recognition. *Advanced Functional Materials* **34**(52), 2411172 (2024). <https://doi.org/10.1002/adfm.202411172>
- [120] Vera, D., García-Díaz, M., Torras, N., Castillo, Ó., Illa, X., Villa, R., Alvarez, M., Martínez, E.: A 3D bio-printed hydrogel gut-on-chip with integrated electrodes for transepithelial electrical resistance (TEER) measurements. *Biofabrication* **16**(3), 035008 (2024). <https://doi.org/10.1088/1758-5090/ad3aa4>
- [121] Hu, F., Yu, D., Dong, B., Gong, X., Li, Z., Zhao, R., Wang, Q., Li, G., Wang, H., Liu, W., et al.: Antibacterial conductive hydrogels with freeze-directed microstructures reinforced by polyaniline-encapsulated bacterial cellulose for flexible sensors. *Chemical Engineering Journal* **512**, 162702 (2025). <https://doi.org/10.1016/j.cej.2025.162702>
- [122] Kim, H., Dutta, S.D., Jeon, M.J., Lee, J., Park, H., Seol, Y., Lim, K.T.: Bioinspired Shape Reconfigurable, Printable, and Conductive "E-Skin" Patch with Robust Antibacterial Properties for Human Health Sensing. *Advanced Functional Materials* **35**(40), 2504088 (2025). <https://doi.org/10.1002/adfm.202504088>
- [123] Huang, D., Qi, J., Gao, S., Yin, L., Qi, H., Zheng, S.: DLP 3D-Printed Conic-Pyramid Hydrogel Sensor for Wearable Devices and Handwritten Fingerprint Recognition. *ACS Applied Materials & Interfaces* **17**(33), 47273–47289 (2025). <https://doi.org/10.1021/acsami.5c07889>
- [124] Wu, K., Li, J., Li, Y., Wang, H., Zhang, Y., Guo, B., Yu, J., Wang, Y.: 3D Printed Silk Fibroin-Based Hydrogels with Tunable Adhesion and Stretchability for Wearable Sensing. *Advanced Functional Materials* **34**(46), 2404451 (2024). <https://doi.org/10.1002/adfm.202404451>
- [125] Zhang, S., Jia, W., Xu, T., Guo, A., Liu, Y., Liu, G., Yang, X., Liu, P., Yang, R., Sui, C.: High-sensitivity wearable sensor based on micro-needle structure design assisted by 3D printing. *Chemical Engineering Journal* **520**, 165966 (2025). <https://doi.org/10.1016/j.cej.2025.165966>
- [126] Liu, Q., Dong, X., Qi, H., Zhang, H., Li, T., Zhao, Y., Li, G., Zhai, W.: 3D printable strong and tough composite organo-hydrogels inspired by natural hierarchical composite design principles. *Nature Communications* **15**(1), 3237 (2024). <https://doi.org/10.1038/s41467-024-47597-7>
- [127] Li, J., Yu, Q., Shen, Z., Wang, D., Gu, G.: Soft 3D Lattice Iontronic Tactile Sensor. *SmartBot* **1**(3), e70002 (2025). <https://doi.org/10.1002/smb2.70002>
- [128] Yang, J., Yang, K., An, X., Fan, Z., Li, Y., Yin, L., Long, Y., Pan, G., Liu, H., Ni, Y.: Highly Flexible, Stretchable, and Compressible Lignin-Based Hydrogel Sensors with Frost Resistance for Advanced Bionic Hand Control. *Advanced Functional Materials* **35**(11), 2416916 (2025). <https://doi.org/10.1002/adfm.202416916>
- [129] Lai, J., Xiao, L., Zhu, B., Xie, L., Jiang, H.: 3D printable and myoelectrically sensitive hydrogel for smart prosthetic hand control. *Microsystems & Nanoengineering* **11**(1), 15 (2025). <https://doi.org/10.1038/s41378-024-00825-y>
- [130] Hui, Y., Yao, Y., Qian, Q., Luo, J., Chen, H., Qiao, Z., Yu, Y., Tao, L., Zhou, N.: Three-dimensional printing of soft hydrogel electronics. *Nature Electronics* **5**(12), 893–903 (2022). <https://doi.org/10.1038/s41928-022-00887-8>

- [131] Yan, Y., Deng, W., Xie, D., Hu, J.: Silk Fibroin Hydrogel for Pulse Waveform Precise and Continuous Perception. *Advanced Healthcare Materials* **14**(4), 2403637 (2024). <https://doi.org/10.1002/adhm.202403637>
- [132] Nezafati, M., Salimiyan, N., Salighehdar, S., Sedghi, R., Dolatshahi-Pirouz, A., Mao, Y.: Facile fabrication of biomimetic and conductive hydrogels with robust mechanical properties and 3D printability for wearable strain sensors in wireless human-machine interfaces. *Chemical Engineering Journal* **509**, 161112 (2025). <https://doi.org/10.1016/j.cej.2025.161112>
- [133] Zhang, Z., Wang, Z., Wang, X., Zhou, X., Zhang, X., Wang, J.: Synthesis of Mimicking Plant Cell Wall-Like Anti-Swelling Hydrogels Based on a "Bottom-Up" Strategy and Their Application in Osmotic Energy Harvesting. *Advanced Functional Materials* **35**(34), 2502946 (2025). <https://doi.org/10.1002/adfm.202502946>
- [134] Zhang, Z., Wang, Z., Wang, X., Zhou, X., Zhang, X., Wang, J.: Synthesis of Mimicking Plant Cell Wall-Like Anti-Swelling Hydrogels Based on a "Bottom-Up" Strategy and Their Application in Osmotic Energy Harvesting. *Advanced Functional Materials* **35**(34), 2502946 (2025). <https://doi.org/10.1002/adfm.202502946>
- [135] Madika, B., Saha, A., Kang, C., Buyantogtokh, B., Agar, J., Wolverson, C.M., Voorhees, P., Littlewood, P., Kalinin, S., Hong, S.: Artificial Intelligence for Materials Discovery, Development, and Optimization. *ACS Nano* **19**(30), 27116–27158 (2025). <https://doi.org/10.1021/acsnano.5c04200>
- [136] Wang, Y., Li, Y., Tang, Z., Li, H., Yuan, Z., Tao, H., Zou, N., Bao, T., Liang, X., Chen, Z., et al.: Universal materials model of deep-learning density functional theory Hamiltonian. *Science Bulletin* **69**(16), 2514–2521 (2024). <https://doi.org/10.1016/j.scib.2024.06.011>
- [137] Hu, J., Li, Q., Fu, N.: Generative AI for Materials Discovery: Design Without Understanding. *Engineering* **39**, 13–17 (2024). <https://doi.org/10.1016/j.eng.2024.07.008>
- [138] Zeni, C., Pinsler, R., Zügner, D., Fowler, A., Horton, M., Fu, X., Shysheya, A., Crabbé, J., Sun, L., Smith, J., et al.: MatterGen: a generative model for inorganic materials design. *arXiv preprint arXiv 2312.03687* (2023). <https://doi.org/10.48550/arXiv.2312.03687>
- [139] Merchant, A., Batzner, S., Schoenholz, S.S., Aykol, M., Cheon, G., Cubuk, E.D.: Scaling deep learning for materials discovery. *Nature* **624**(7990), 80–85 (2023). <https://doi.org/10.1038/s41586-023-06735-9>
- [140] Xu, S., Xia, X., Yu, Q., Parakh, A., Khan, S., Megidish, E., You, B., Hemmerling, B., Jayich, A., Beck, K., et al.: 3D-printed micro ion trap technology for quantum information applications. *Nature* **645**(8080), 362–368 (2025). <https://doi.org/10.1038/s41586-025-09474-1>
- [141] Shi, i., Kim, S., Li, P., Dong, F., Yang, C., Nam, B., Han, C., Eig, E., Shi, L.L., Niu, S., et al.: Active biointegrated living electronics for managing inflammation. *Science* **384**(6699), 1023–1030 (2024). <https://doi.org/10.1126/science.adl1102>
- [142] Nakamura, K., Di Caprio, N., Burdick, J.A.: Engineered Shape-Morphing Transitions in Hydrogels Through Suspension Bath Printing of Temperature-Responsive Granular Hydrogel Inks. *Advanced Materials* **36**(47), 2410661 (2024). <https://doi.org/10.1002/adma.202410661>
- [143] Cao, R., Chen, G., Wang, L., Wang, W., Ni, C., Xia, Z., Hu, A., Hu, W., Lin, H., Qian, P., et al.: 4D Printed Hydrogel Expanders for Personalized and Accelerated Soft Tissue Regeneration. *Advanced Materials*, e12662 (2025). <https://doi.org/10.1002/adma.202512662>
- [144] Ni, C., Zhang, C., Qin, Z., Ke, Q., Wu, B., Zhuoruo, X., Sun, Y., Fu, Q., Chen, D., Zheng, N., et al.: 4D printing of trigger-free shape-memory hydrogels towards self-adaptive substrates for bioelectronics. *Nature Communications* **17**, 677 (2026). <https://doi.org/10.1038/s41467-025-67323-1>
- [145] Lin, W., Zhang, J., Pan, G., Lin, Y., Chen, D., Lu, J., Li, J., Huang, J., Li, Z., Lin, X., et al.: Multifunctional Wide-Temperature Threshold Conductive Eutectic Hydrogel Sensor for Shoulder Pain Monitoring and Photothermal Therapy. *Advanced Functional Materials* **35**(49), e09779 (2025). <https://doi.org/10.1002/adfm.202509779>
- [146] Zhianmanesh, M., Khodaei, A., Crago, M., Lotz, O., Naficy, S., Dehghani, F., Bilek, M., Amin Yavari, S., Akhavan, B.: Universal Method for Covalent Attachment of Hydrogels to Diverse Polymeric Surfaces for Biomedical Applications. *Advanced Materials* **38**(1), e03524 (2025). <https://doi.org/10.1002/adma.202503524>
- [147] Ye, X., Chen, Y., Lv, C., Ying, Y., Ping, J., Pan, J., Lan, L.: In situ formed hydrogels for soft bioelectronics. *Materials Horizons* **12**(22), 9537–9555 (2025). <https://doi.org/10.1039/D5MH01356A>
- [148] Xu, W., Gu, Y., Xia, W., Yu, A., Fan, W., Qian, S., Shu, Q., Liu, B., Li, Y.: Zwitterionic Surfactant Enhanced Stable Hydrogels for Epidermal Sensors and External Contact Object Perception. *ACS Sensors* **10**(7), 5199–5208 (2025). <https://doi.org/10.1021/acssensors.5c01319>
- [149] Wang, J., Xu, Y., Li, S., Tang, L., Li, X., Song, J., Liu, Y.: Physical entanglement improves the anti-adsorption and super-lubricity properties of polyacrylamide-based

- hydrogels for biomedical applications. *Advanced Composites and Hybrid Materials* **8**, 208 (2025). <https://doi.org/10.1007/s42114-025-01267-4>
- [150] Sun, Q., Hong, K., Fan, L., Zhang, X., Wu, T., Du, J., Zhu, Y.: Bioabsorbable Zwitterionic Hydrogels Achieving Excellent Protein Repulsion and Cell Adhesion. *Chemistry of Materials* **35**(21), 9208–9224 (2023). <https://doi.org/10.1021/acs.chemmater.3c01923>
- [151] Gu, Y., Luo, Y., Guo, Q., Yu, W., Li, P., Wang, X., Ye, T., Chang, H., Yuan, W., Wu, H., et al.: Empowering Human-Machine Interfaces: Self-Powered Hydrogel Sensors for Flexible and Intelligent Systems. *Advanced Functional Materials*, e09085 (2025). <https://doi.org/10.1002/adfm.202509085>
- [152] Kunwar, P., Xiong, Z., Zhu, Y., Li, H., Filip, A., Soman, P.: Hybrid Laser Printing of 3D, Multiscale, Multimaterial Hydrogel Structures. *Advanced Optical Materials* **7**(21), 1900656 (2019). <https://doi.org/10.1002/adom.201900656>